Analysis of regional seismograms and 3D synthetic seismograms for the 2016-01-24 $M_{\rm w}$ 7.1 Iniskin earthquake in southern Alaska

Carl Tape, ctape@alaska.edu

Geophysical Institute, University of Alaska Fairbanks

Version 1: November 3, 2016
Version 2: November 6, 2016
Version 3: November 6, 2016
Version 4: November 29, 2016
Version 5: December 6, 2016
This document is downloadable as a pdf via the link listed in *Tape* (2016b).

Contents

List of Tables

List of Figures

Overview

I perform two analyses to identify cases of seismogram clipping or other problems (e.g., data gaps) for the 2016-01-24 M_w 7.1 Iniskin, Alaska, earthquake. The first analysis is a comparison of synthetic and observed seismograms: three-component, displacement seismograms filtered between periods 4–80 s. The subset of 141 stations is limited to an oblique rectangular region that is 1200 km × 600 km (Figures 1 and 2) and used in a seismic wavefield simulation with a three-dimensional seismic velocity model. I identify 60 out of 141 stations that are suspected of clipping or other problems. Of the 81 good stations, only 8 are within 250 km of the Iniskin epicenter, and all 8 stations are outside of Cook Inlet basin, which strongly amplifies ground motion (both in data and in synthetics). The second, much simpler, analysis is to identify clipping based on the maximum counts on the waveforms. The max-counts approach reveals general agreeement with the classification based on long-period data and synthetics. The analysis suggests that (1) some recorded waveforms that exceed clipping levels may still be usable for some modeling purposes, and (2) some recorded waveforms that appear to be suitable for modeling purposes should probably be discarded due to clipping at high frequencies. The identification of suspected stations, along with the waveform comparisons, may help network operators assess the possibility of unexpected performance during the M_w 7.1 slab earthquake.

Table 1: Number of stations in each category, separated by epicentral distance. All 141 stations are within the simulation region of Figure 1.

	$\Delta < 250$ km	$\Delta \geq 250$ km	all distances
"good" stations	8	73	81
"bad" stations	40	20	60
all stations	48	93	141

1 Synthetic seismograms

Synthetic seismograms were calculated from a wavefield simulation in a 3D seismic velocity model for Alaska. The details of the wavefield simulation are in *Tape* (2016a) and copied in Section 1.1. The synthetics from this report have some minor modifications, discussed in Section 1.2. The simulation region is shown in Figure 1; it is the same simulation used in *Tape* (2014) for the 1964-03-28 M_w 9.2 earthquake.

1.1 Description of wavefield simulation [copy of notes in *Tape* (2016a)]

For a zoomed-in version of this movie, please see `https://youtu.be/KdiETNfyaUo`
Also: `http://www.giseis.alaska.edu/input/carl/research/earthquakes/iniskin.html`
This is a 1200 km by 600 km oblique view of southern Alaska; some cities are labeled for reference: Kodiak (K), Homer (H), Kenai (K), Seward (S), Anchorage (A), Palmer (P), Cantwell (C), Nenana (N), and Fairbanks (F). This computer simulation shows a surface view of three-dimensional earthquake wave propagation of the magnitude 7.1 Iniskin earthquake on January 24, 2016; the epicenter is represented by the blue ball. The earthquake originated at about 120 km depth, within the subducting Pacific plate. The earthquake was felt over much of Alaska, from Anchorage to Fairbanks. The simulation demonstrates the complexity of the seismic wavefield that arises

from realistic models of Earth structure. We see a striking effect due to the slow wave speeds within Cook Inlet sedimentary basin. The simulation was performed on the high-performance computing cluster at the University of Alaska Fairbanks, Research Computing Systems. The 3D wave propagation code is called SPECFEM3D (*Komatitsch et al.*, 2004). Credit: Carl Tape

A MESH. The finite element mesh was generated with the GEOCUBIT software (Casarotti), an extension of CUBIT software to geological structures. The unstructured mesh is designed to optimally handle slow wave speeds near the surface and faster wave speeds in the upper mantle. The mesh contains 4,696,704 hexahedral elements that are largest at the bottom of the mesh, at 400 km below sea level, and smallest at the topographic surface. There are 312 million gridpoints in the mesh; the gridpoint spacing at the surface is about 200 m. The topographic detail that is visible in the movie is the actual top surface of the mesh. Denali is within the simulation region. (You can see places where the topography influences the wavefield.)
Credits: Ulrika Cahayani Miller and Emanuele Casarotti

B STRUCTURE MODEL. The Earth structure model is that of *Eberhart-Phillips et al.* (2006), with an embedded model of Cook Inlet basin (*Shellenbaum et al.*, 2010). The effects of Cook Inlet basin (west of Anchorage) on the wavefield are prominent. The ocean layer is ignored but is not expected to influence the wavefield at these periods. Active faults of Alaska, including the Denali fault (M_{w} 7.9 on 2003-11-02), are plotted in white (*Koehler et al.*, 2012).

The model does not incorporate the shallowest structural models, such as the USGS Vs30 maps, which provide the shear-wave velocities in the uppermost 30 m (`http://earthquake.usgs.gov/hazards/apps/vs30/predefined.php`). The structure of Cook Inlet basin is modeled as the generic basin model of *Brocher* (2008). As far as I know, there is no publicly available model of the 1D or 3D seismic structure of Cook Inlet basin. (If there is, please let me know!)

C SOURCE MODEL. The earthquake is represented by a simple point-source model known as a moment tensor. The source-time function is approximated as a simple Gaussian function with a half duration of 2 seconds. At present (2016-01-26), seismologists are working to estimate a more complex and accurate source model for this earthquake; we anticipate using such a source model for future simulations.
Credits: Vipul Silwal and the Alaska Earthquake Center

D COMPUTATION. The simulation used a time step of 0.006 s and iterated 44,000 time steps. The calculation took 10.0 hours on 240 cores (2400 CPU-hours) on the high-performance computing cluster at the University of Alaska Fairbanks, Research Computing Systems.

E WHAT YOU SEE. The scalar field that is plotted is the simulated vertical component of ground velocity. The simulation keeps track of all three components of ground motion. (Alternatively one could plot ground displacement or acceleration.) The two pulses at the beginning correspond to the P wave and the S wave, which is followed by surface waves.

1.2 Synthetic seismograms in this report

The synthetic seismograms presented in this report are slightly different from those computed to make the movie discussed above. First, we use the origin time, hypocenter, and moment tensor from the GCMT catalog (*Ekström et al.*, 2012). Second, after comparing observed and synthetic seismograms, we apply a magnitude correction to the synthetic seismograms. The uncorrected magnitude is M_{w} 7.11. After cutting the scalar seismic moment in half, the corrected moment magnitude is M_{w} 6.91. (Note that the seismogram displacement is proportional to moment M_0.)

At this stage, it is unclear why a lower magnitude is needed to fit the observed seismograms. One possibility could be that our simulation does not consider attenuation, which could be strong within Cook Inlet basin and other regions. Turning on attenuation would result in a larger magnitude in order to fit the observed seismic amplitudes. However, we are analyzing relatively long periods (4–80 s), where we might expect the effects of attenuation to be less pronounced. Another possibility for the magnitude correction is based on the source duration. Based on empirical scaling between moment and half duration, one would expect a half duration of 9.36 s for a point source with the magnitude of the Iniskin earthquake (and 7.43 s for the halved-moment earthquake). We used a half duration of 2.0 s in order to examine the influence of the regional structures on the shorter-period wavefield. It is possible that a longer source duration, or a more realistic finite-source model, would produce synthetic seismograms that would better match the observed amplitudes.

2 Recorded seismograms

Almost all seismograms and station metadata were retrieved from the IRIS Data Management Center. Seismograms were processed using ObsPy (*Beyreuther et al.*, 2010; *Megies et al.*, 2011; *Krischer et al.*, 2015). The main steps involved deconvolving of the instrument response to obtain velocity seismograms, rotating to E and N to account for the sensor azimuth, detrending, integrating to displacement, then bandpass filtering over the period range 4–80 s.

We also include seismograms from the Alaska Pipeline pump stations. The seismograms are retrieved from the Alaska Earthquake Center.

3 Analysis

3.1 Analysis #1: Comparison of long-period data and synthetics

My approach was to plot record sections with recorded and synthetic seismograms superimposed. My first goal was to confirm that at least some synthetic seismograms provided reasonable fits to observed seismograms. This provided a qualitative (and quantitative, if desired) check that the source model and 3D structure model could adequately model the seismic wavefield at periods 4–80 s. A comparison between recorded and synthetic peak displacements is shown in Figure 10.

With faith in the synthetic seismograms, I then identified the observed seismograms that exhibited suspicious deviations from synthetic seismograms. In the text below, I label each station simply as one of these:

- **bad**: stations having major discrepancies between recorded and 3D synthetic seismograms on at least one of three components (Z, E, N) for displacements filtered 4–80 s. The most likely source of the discrepancies is clipping from the M_{w} 7.1 earthquake, but there could be other factors, too.

- **good**: stations having no major discrepancies between recorded and 3D synthetic seismograms. It is still possible that there are problems at these stations, but they are not apparent in this analysis.

  The identification of "major discrepancies" is primarily determined from the earlier portion of the seismogram, prior to the surface waves. For example, recorded seismograms at FLATS (network XV) stations overlying Nenana basin are only fit by synthetic seismograms for the pre-surface wave arrivals. Although there are major discrepancies between recorded and synthetic waveforms, the discrepancies can be attributed to overly simple synthetics (not to the data), which, in turn, are due to the lack of any Nenana basin in the 3D model.

Keep in mind that for many purposes—e.g., volcanic monitoring for hypocentral location of small events—the station response at 4–80 s may not be so important. However, it is possible that a problematic response identified at 4–80 s could be indicative of a corrupted response at other frequencies, too.

I grouped the stations based on epicentral distance (Δ) less than or greater than 250 km (Table 1). This is an arbitrary choice.

3.2 Analysis #2: Check for clipping threshold

In Tables 6 and 7, I list the maximum of the absolute value counts on each channel for each station. For each station, the max value across all components is compared against a threshold value for the digitizer. I have assumed that all stations use a 24-bit digitizer except for GSN stations (COLA, KDAK), which use 26-bit digitizers. (Please email me if the number of bits for your digitizer is incorrectly listed.) The threshold value is $q = |2^{N-1}|$, where N is the number of bits in the digitizer.

As a proxy for the squareness of waves, I list the number of timesteps for which $|c(t)| > 0.8q$, where $c(t)$ is the raw seismogram in counts. This allows one to easily identify clipping values that are a single spike versus a set of squared waveforms.

3.3 Summary points

1. Figure 2 shows the spatial pattern of good (black) and bad (red) stations inside the simulation region. The overall pattern shows a "bad" region that extends from the earthquake 500 km eastward to Cordova and northward to approximately 62.5° latitude. The pattern is more apparent when taking into account the following anomalies:

   (a) All volcano observatory stations (network AV; all of which were $\Delta \leq 250$ km) were bad (Table 5), including those that were in proximity to good stations. For example, the SALMON and TA sites west of Redoubt were good, whereas the AV sites further to the north, on the more-distant Spurr, were not.

   (b) The closest pump stations, along the Richardson Highway south of Delta (Figure 2), were bad: PS09, PS10, PS11, PS12, VMT, with distances $\Delta = 400$–600 km (Table 5). Only the most distant pump stations inside the simulation region were good: PS07 and PS08, with distances $\Delta > 600$ km. Note that pump stations have strong-motion sensors as well.

   (c) AT.PMR, at distance 305 km and azimuth 46° (Table 2), is good[1], and it is surrounded by bad stations (Figure 2).

   (d) AK.BGLC, to the east and at distance 559 km, is bad[2] is surrounded by good stations (Figure 2).

2. The 81 good stations are shown in Figures 5 and 7. Keep in mind that some of these recordings may still be corrupted, but from this analysis I cannot say that they are bad.

3. The 60 bad stations are shown in Figure 9. Keep in mind that some of these recordings may still be scientifically useful, especially a shorter periods. (Use caution!)

4. Within 250 km of the M_{w} 7.1 Iniskin earthquake, most (40/48) broadband stations were bad, including all stations overlying the Cook Inlet basin, where amplification of ground motion occurred.

[1] Raw waveforms indicate that AT.PMR might be clipped; see values in Table 6.
[2] Raw waveforms indicate that AK.BGLC might be clipped; see values in Table 7.

There were 20 stations from SALMON (network ZE; *Tape et al.* (2015)) operating at the time of the earthquake; all but ZE.GOOS were within 250 km of the epicenter. 16/20 were bad (Table 5), 3/20 were good, and 1/20 (ZE.WFLW) was outside the simulation region. All SALMON stations are direct-burial posthole sensors.

5. The 8/48 good stations within 250 km include (Figure 5): 4 from Transportable Array (TA.P18K, TA.O18K, TA.O19K, TA.N19K), 3 from SALMON (ZE.WFLS, ZE.HLC5, ZE.HLC3), and one from GSN (II.KDAK.10).

   All 8 good stations $\Delta \leq 250$ km were west of Cook Inlet basin and were either direct-burial posthole sensors or borehole sensors (Table 2).

   The closest TA stations were bad: TA.O20K (52 km) and TA.Q19K (94 km) (Table 4).

6. There were several bad stations at epicentral distances $\Delta \geq 250$ km (Table 4). It is unclear why some stations were bad whereas nearby stations were good. Factors such as sensor type, installation type, site conditions, influence of 3D structures (such as nearby basins), and source radiation pattern need to be considered.

7. For the two GSN stations in the simulation region (IU.COLA at 636 km, II.KDAK at 223 km), both COLA sensors (location 00 in borehole, location 10 at surface) were good[3], the II.KDAK.10 surface sensor was good, and the II.KDAK.00 borehole sensor was (barely) bad (Figure 9, Part 5)[4]. Note that GSN stations also have strong motion sensors.

8. The good/bad classification based on long-period data and synthetics has general agreement with a clipping classification based on max-count values, though there are some differences.

   Among the good stations (Table 6), several exceeded (or were very close to) the threshold. This means that the long-period waveform comparisons look good, but the seismogram exceeded the clipping threshold. One would want to be very cautious about using these waveforms.

   Among the bad stations (Table 7), only AK.SWD and several AV stations did not exceed the threshold. Natalia Rupport wrote: "SWD may have had a bad component. The sensor was replaced in August."

9. The peak ground displacement (periods 4–80 s), in both the data and synthetics and on each component, occurred due north of the earthquake, at SALMON station ZE.HLC3 (Figure 10).

10. One of the largest real anomalies between data and synthetics is for the FLATS stations (network XV; *Tape and West* (2014)) that are within Nenana basin; see Figure 7, Parts 2-3. Since there is no model of Nenana basin within our 3D velocity model in the simulation, the synthetics provide a poor approximation to the real seismograms.

    The amplitude anomaly for FLATS stations are also evident in Figures 10 and 11: see stations F1TN, F2TN, F3TN, F4TN, and F5MN on the horizontal components.

11. Stations to the east exhibit higher amplitudes and extended duration, as shown in Figure 7, Parts 8–10. These longer codas are in the synthetics, too, though not as pronounced as in the data. Most of the closer stations at these azimuths are bad (Figure 2). It is unclear what the origin of the high amplitudes to the east are. Possibly the source radiation and the effects of Cook Inlet basin (or some other 3D structure) are influential.

[3]The raw waveforms for COLA.10 show that the seismogram clearly clipped; see values in Table 6. Nevertheless, I identify it as a "good" station based on the comparison with synthetics.

[4]The raw waveforms for KDAK.10 reveal only a few points that exceeded the clipping thredhold; see values in Table 7.

12. 3D synthetic seismograms provide a useful tool for analyzing recorded seismograms for problems such as clipping. The better the source model and 3D structural model, the more useful the synthetic seismograms.

    One should also perform the much simpler analysis of comparing the max-count values on the raw seismograms with thresholds from the digitizers, as in Tables 6 and 7.

3.4 Take-away points and questions

1. The goal is to determine which seismograms are not showing true ground motion. Clipping—in the extreme form of squared waveforms that exceed the clipping threshold value of the digitizer—is one example. There are subtler cases of clipping where possibly part of a waveform—and at a particular frequency range—is accurate while another part is not.

2. How reliable is a waveform's shape and amplitude if it has been clipped? In other words, can it still be filtered at some period range and be used for modeling purposes?

3. Why does clipping occur at one station but not the other? Can we hope to understand this?

4. It seems possible to quantify the severity of clipping based on the number of points that exceed some fraction of the clipping threshold. (The clipping threshold will depend on the number of bits of the digitizer.) This could be useful in an operational setting, where rapid estimation of large-magnitude events is important.

4 Summary of revisions to report

- **Version 2.**
  Almost all waveforms (all except pump station stations) are now extracted from IRIS DMC and processed using ObsPy. This led to revised results for KDAK, COLA, and POKR, among others. The revised results could be explained by two possibilities. (1) The metadata used in Version 1, which were obtained from the Alaska Earthquake Center (IRIS dataless seed → Antelope database) via Matlab, could be different from the metadata obtained from IRIS via ObsPy. (2) The deconvolution used in Version 1 could have produced incorrect results, at least at some stations.

  The sensor types are no longer visible in the tables (e.g., Table 2), since we do not have this information in the sac files extracted from IRIS. I may be able to include this information in a future version.

  There are some discrepancies between waveform availability from IRIS and from AEC. I did not thoroughly examine these, but I did notice that some stations (e.g., TA.J25K, AK.RAG, AK.TBL, AK.SSN) are zero-amplitude data streams from AEC but are not available from IRIS. Hence these stations are categorized as bad stations in Version 1 but are not included in Version 2.

- **Version 3.**
  In Version 2, Figure 2 was missing the beachball and also the stations outside the simulation region.

- **Version 4.**
  - Added the basin contours to Figure 2
  - Added the zoom-in map in Figure 3
  - Added the sensor types in the tables (e.g., Table 2)
  - Added the record section in Figure 12

- **Version 5.**
  - Added an analysis based on max-count values from raw seismograms: Tables 6 and 7 and Section 3.2
  - Added Section 3.4
  - Added Table 1

Acknowledgments

Thanks to the following people for providing feedback on earlier versions of this report: Natalia Ruppert, Bob Busby, Tyler Storm, Pete Davis, Katrin Hafner, Geoff Abers, Geoff Bainbridge, and Noel Barstow. Thanks to Vipul Silwal, Celso Alvizuri, and Lion Krischer for support with data retrieval and processing with ObsPy.

References

Beyreuther, M., R. Barsch, L. Krischer, T. Megies, Y. Behr, and J. Wassermann (2010), ObsPy: A Python toolbox for seismology, *Seis. Res. Lett.*, *81*(3), 530–533, doi:10.1785/gssrl.81.3.530.

Brocher, T. M. (2008), Compressional and shear-wave velocity versus depth relations for common rock types in northern California, *Bull. Seis. Soc. Am.*, *98*(2), 950–968.

Eberhart-Phillips, D., D. H. Christensen, T. M. Brocher, R. Hansen, N. A. Ruppert, P. J. Haeussler, and G. A. Abers (2006), Imaging the transition from Aleutian subduction to Yakutat collision in central Alaska, with local earthquakes and active source data, *J. Geophys. Res.*, *111*, B11303, doi:10.1029/2005JB004240.

Ekström, G., M. Nettles, and A. M. Dziewoński (2012), The global GCMT project 2004–2010: Centroid-moment tensors for 13,017 earthquakes, *Phys. Earth Planet. Inter.*, *200-201*, 1–9, doi:10.1016/j.pepi.2012.04.002.

Koehler, R. D., R.-E. Farrell, P. A. C. Burns, and R. A. Combelick (2012), Quaternary faults and folds in Alaska: A digital database, Alaska Div. Geol. Geophys. Surv. Miscellaneous Publication 141, 31 p., 1 sheet, scale 1:3,700,000.

Komatitsch, D., Q. Liu, J. Tromp, P. Süss, C. Stidham, and J. H. Shaw (2004), Simulations of ground motion in the Los Angeles basin based upon the spectral-element method, *Bull. Seis. Soc. Am.*, *94*(1), 187–206, doi:10.1785/0120030077.

Krischer, L., T. Mengies, R. Barsch, M. Beyreuther, T. Lecocq, C. Caudron, and J. Wassermann (2015), ObsPy: a bridge for seismology into the scientific Python ecosystem, *Computational Science & Discovery*, *8*(1), 014003, doi:10.1088/1749-4699/8/1/014003.

Megies, T., M. Beyreuther, R. Barsch, L. Krischer, and J. Wassermann (2011), ObsPy – What can it do for data centers and observatories, *Annals. Geophy.*, *54*(1), 47–58, doi:10.4401/ag-4838.

Shellenbaum, D. P., L. S. Gregersen, and P. R. Delaney (2010), Top Mesozoic unconformity depth map of the Cook Inlet Basin, Alaska, doi:10.14509/21961, Alaska Div. Geol. Geophys. Surv. Report of Investigation 2010-2, 1 sheet, scale 1:500,000, available at `http://www.dggs.alaska.gov/pubs/id/21961` (last accessed 2016-10-30).

Tape, C. (2014), Seismic wavefield simulations of earthquakes within a complex crustal model for Alaska, Abstract presented at the 2014 SSA Annual Meeting, Anchorage, Alaska, April 30 - May 2.

Tape, C. (2016a), Magnitude 7.1 Alaska earthquake on January 24, 2016 (computer simulation), YouTube movie at `https://youtu.be/E4RYnpIOoPw` (last accessed 2016-10-08).

Tape, C. (2016b), Analysis of regional seismograms and 3D synthetic seismograms for the 2016-01-24 Mw 7.1 Iniskin earthquake in southern Alaska, ScholarWorks@UA at `http://hdl.handle.net/11122/6983` (last accessed November 3, 2016).

Tape, C., and M. E. West (2014), Fault Locations and Alaska Tectonics from Seismicity, International Federation of Digital Seismograph Networks. Other/Seismic Network. `doi:10.7914/SN/ZE_2015`.

Tape, C., D. H. Christensen, and M. M. Driskell (2015), Southern Alaska Lithosphere and Mantle Observation Network, International Federation of Digital Seismograph Networks. Other/Seismic Network. `doi:10.7914/SN/ZE_2015`.

Table 2: 81 stations with "good" seismograms for the M_w 7.1 Iniskin earthquake. The list is sorted by epicentral distance: 8 are <250 km, 73 are ≥250 km. These seismograms are shown in Figures 5 and 7.

net	sta	loc	distance	azimuth	response_file
TA	O19K		76.8 km	310.7 deg	Nanometrics Trillium 120 Sec Response/Quanterra
ZE	HLC3		94.8 km	359.8 deg	Nanometrics Trillium 120 Sec PH Response/Quanter
TA	O18K		109.4 km	276.9 deg	Nanometrics Trillium 120 Sec Response/Quanterra
TA	P18K		117.7 km	251.0 deg	Nanometrics Trillium 120 Sec Response/Quanterra
ZE	HLC5		118.2 km	339.4 deg	Nanometrics Trillium 120 Sec PH Response/Quanter
TA	N19K		136.2 km	331.0 deg	Nanometrics Trillium 120 Sec Response/Quanterra
ZE	WFLS		152.9 km	328.2 deg	Nanometrics Trillium 120 Sec PH Response/Quanter
II	KDAK	10	222.7 km	169.4 deg	Nanometrics Trillium 120Posthole BB Seismometer
AT	OHAK		281.5 km	180.2 deg	STS-2/Trident
AT	PMR		305.4 km	46.0 deg	STS-2/Trident
AK	PPLA		355.3 km	8.9 deg	Nanometrics Trillium 240 Sec Response sn400 and
AK	SII		359.4 km	189.0 deg	Nanometrics Trillium 240 Sec Response sn400 and
TA	Q23K		392.9 km	92.2 deg	Nanometrics Trillium 120 Sec Response/Quanterra
AT	MID		393.0 km	92.2 deg	STS-2/Trident
AK	CAST		413.6 km	8.2 deg	Nanometrics Trillium 240 Sec Response sn400 and
AK	EYAK		426.8 km	74.7 deg	Guralp CMG3T_120sec/Quanterra 330 LinearPhase B
AK	TRF		441.5 km	19.7 deg	Streckeisen STS-2 G3/Quanterra 330 Linear Phase
AK	KTH		441.6 km	15.3 deg	Nanometrics Trillium 240 Sec Response sn400 and
AK	SGA		456.1 km	75.5 deg	Nanometrics Trillium 240 Sec Response sn400 and
AK	CHI		459.3 km	198.7 deg	Nanometrics Trillium 240 Sec Response sn400 and
AK	RND		469.7 km	28.0 deg	Streckeisen STS-2 G3/Quanterra 330 Linear Phase
AK	GOAT		482.8 km	75.3 deg	Nanometrics Trillium 240 Sec Response sn400 and
AK	KAI		496.3 km	83.9 deg	Nanometrics Trillium 120 Sec Response/Quanterra
AK	BMR		496.7 km	70.4 deg	Nanometrics Trillium 120 Sec Response/Quanterra
AK	MCK		499.1 km	25.4 deg	Nanometrics Trillium 120 Sec Response/Quanterra
AK	BPAW		499.3 km	12.9 deg	Nanometrics Trillium 240 Sec Response sn400 and
AK	HMT		505.8 km	78.7 deg	Nanometrics Trillium 120 Sec Response/Quanterra
TA	N25K		516.6 km	62.7 deg	Nanometrics Trillium 120 Sec Response/Quanterra
AK	NICH		521.5 km	80.0 deg	Nanometrics Trillium 240 Sec Response sn400 and
AK	SUCK		531.8 km	82.0 deg	Nanometrics Trillium 120 Sec Response/Quanterra
AK	BWN		534.9 km	21.2 deg	Nanometrics Trillium 120 Sec Response/Quanterra
AK	BERG		537.1 km	78.2 deg	Nanometrics Trillium 240 Sec Response sn400 and
AK	PAX		549.7 km	45.9 deg	Nanometrics Trillium 120 Sec Response/Quanterra
AK	GLB		550.8 km	65.9 deg	Nanometrics Trillium 240 Sec Response sn400 and
AK	GRIN		557.5 km	79.6 deg	Streckeisen STS-2 G3/Quanterra 330 Linear Phase
AK	KHIT		562.2 km	77.8 deg	Nanometrics Trillium 240 Sec Response sn400 and
AK	VRDI		563.5 km	68.8 deg	Nanometrics Trillium 240 Sec Response sn400 and
XV	FNN2		573.3 km	18.7 deg	Nanometrics Trillium 120 Sec PH Response/Quanter
XV	FNN1		577.1 km	19.7 deg	Nanometrics Trillium 120 Sec PH Response/Quanter
XV	FAPT		577.5 km	20.4 deg	Nanometrics Trillium 120 Sec PH Response/Quanter
AK	NEA2		582.1 km	20.2 deg	Nanometrics Trillium 120 Sec Response/Quanterra
XV	FPAP		583.6 km	20.0 deg	Nanometrics Trillium 120 Sec PH Response/Quanter
AK	WAX		584.1 km	77.9 deg	Nanometrics Trillium 120 Sec Response/Quanterra
XV	F8KN		585.1 km	15.8 deg	Nanometrics Trillium 120 Sec PH Response/Quanter
XV	F1TN		586.7 km	19.6 deg	Nanometrics Trillium 120 Sec PH Response/Quanter
AK	WRH		591.1 km	24.9 deg	Nanometrics Trillium 240 Sec Response sn400 and
XV	F2TN		592.8 km	19.5 deg	Nanometrics Trillium 120 Sec PH Response/Quanter
XV	F7TV		596.0 km	15.9 deg	Nanometrics Trillium 120 Sec PH Response/Quanter
XV	FTGH		596.9 km	20.8 deg	Nanometrics Trillium 120 Sec PH Response/Quanter
XV	F3TN		598.9 km	19.1 deg	Nanometrics Trillium 120 Sec PH Response/Quanter
XV	F6TP		601.9 km	17.0 deg	Nanometrics Trillium 120 Sec PH Response/Quanter
XV	F4TN		605.2 km	18.9 deg	Nanometrics Trillium 120 Sec PH Response/Quanter
XV	F5MN		610.1 km	18.5 deg	Nanometrics Trillium 120 Sec PH Response/Quanter
AK	PTPK		614.6 km	70.3 deg	Nanometrics Trillium 240 Sec Response sn400 and
AK	CCB		614.8 km	25.1 deg	Nanometrics Trillium 240 Sec Response sn400 and
AK	HDA		614.8 km	29.7 deg	Nanometrics Trillium 120 Sec Response/Quanterra
AK	KIAG		615.8 km	73.1 deg	Nanometrics Trillium 240 Sec Response sn400 and
AK	BAL		618.3 km	71.9 deg	Nanometrics Trillium 120 Sec Response/Quanterra
AT	MENT		621.5 km	51.1 deg	Trillium-240/Trident
TA	M26K		627.4 km	57.5 deg	Streckeisen STS-5A/Quanterra 330 Linear Phase Co
AK	RIDG		628.2 km	41.4 deg	Nanometrics Trillium 120 Sec Response/Quanterra
PS	PS08		630.4 km	29.4 deg	cmg3esp_60sec+q330_lb100c@50
TA	I23K		634.3 km	16.8 deg	Streckeisen STS-5A/Quanterra 330 Linear Phase Co
TA	TCOL		635.7 km	23.8 deg	Streckeisen STS-4B/Quanterra 330 Linear Phase Co
IU	COLA	00	635.7 km	23.8 deg	Geotech KS-54000Borehole Seismometer
IU	COLA	10	635.7 km	23.8 deg	Streckeisen STS-2 High-gain
IU	COLA	10	635.7 km	23.8 deg	Streckeisen STS-2 High-gain
AK	MDM		636.1 km	22.0 deg	Nanometrics Trillium 120 Sec Response/Quanterra
TA	L26K		642.7 km	51.2 deg	Nanometrics Trillium 120 Sec Response/Quanterra
AK	DOT		651.4 km	44.3 deg	Nanometrics Trillium 120 Sec Response/Quanterra
AK	BARN		655.3 km	72.1 deg	Nanometrics Trillium 240 Sec Response sn400 and
TA	POKR		669.2 km	24.2 deg	Nanometrics Trillium 240 Sec Response sn400 and
TA	POKR	01	669.2 km	24.2 deg	Streckeisen STS-4B/Quanterra 330 Linear Phase Co
PS	PS07		670.4 km	20.3 deg	cmg3esp_30sec+q330_lb100c@50
AK	SCRK		677.3 km	42.0 deg	Nanometrics Trillium 120 Sec Response/Quanterra
TA	M27K		679.3 km	59.8 deg	Nanometrics Trillium 120 Sec Response/Quanterra
CN	YUK2		712.5 km	66.3 deg	Guralp CMG3ESP_60sec/Taurus Standard 47k
TA	L27K		712.5 km	53.9 deg	Streckeisen STS-5A/Quanterra 330 Linear Phase Co
CN	BVCY		731.0 km	60.7 deg	Guralp CMG3ESP_NSN/Taurus Standard 47k
TA	H24K		731.5 km	19.7 deg	Streckeisen STS-5A/Quanterra 330 Linear Phase Co
CN	YUK3		732.5 km	66.6 deg	Guralp CMG3ESP_60sec/Taurus Standard 47k

Table 3: Same as Table 2, but here the stations are grouped by network. The lower set of AK stations are posthole sensors (MCK, PAX, NEA2, HDA, RIDG, MDM, DOT, SCRK).

net	sta	loc	distance	azimuth	response_file
AK	BAL		618.3 km	71.9 deg	Nanometrics Trillium 120 Sec Response/Quanterra
AK	BARN		655.3 km	72.1 deg	Nanometrics Trillium 240 Sec Response sn400 and
AK	BERG		537.1 km	78.2 deg	Nanometrics Trillium 240 Sec Response sn400 and
AK	BMR		496.7 km	70.4 deg	Nanometrics Trillium 120 Sec Response/Quanterra
AK	BPAW		499.3 km	12.9 deg	Nanometrics Trillium 240 Sec Response sn400 and
AK	BWN		534.9 km	21.2 deg	Nanometrics Trillium 120 Sec Response/Quanterra
AK	CAST		413.6 km	8.2 deg	Nanometrics Trillium 240 Sec Response sn400 and
AK	CCB		614.8 km	25.1 deg	Nanometrics Trillium 240 Sec Response sn400 and
AK	CHI		459.3 km	198.7 deg	Nanometrics Trillium 240 Sec Response sn400 and
AK	EYAK		426.8 km	74.7 deg	Guralp CMG3T_120sec/Quanterra 330 LinearPhase B
AK	GLB		550.8 km	65.9 deg	Nanometrics Trillium 240 Sec Response sn400 and
AK	GOAT		482.8 km	75.3 deg	Nanometrics Trillium 240 Sec Response sn400 and
AK	GRIN		557.5 km	79.6 deg	Streckeisen STS-2 G3/Quanterra 330 Linear Phase
AK	HMT		505.8 km	78.7 deg	Nanometrics Trillium 120 Sec Response/Quanterra
AK	KAI		496.3 km	83.9 deg	Nanometrics Trillium 120 Sec Response/Quanterra
AK	KHIT		562.2 km	77.8 deg	Nanometrics Trillium 240 Sec Response sn400 and
AK	KIAG		615.8 km	73.1 deg	Nanometrics Trillium 240 Sec Response sn400 and
AK	KTH		441.6 km	15.3 deg	Nanometrics Trillium 240 Sec Response sn400 and
AK	NICH		521.5 km	80.0 deg	Nanometrics Trillium 240 Sec Response sn400 and
AK	PPLA		355.3 km	8.9 deg	Nanometrics Trillium 240 Sec Response sn400 and
AK	PTPK		614.6 km	70.3 deg	Nanometrics Trillium 240 Sec Response sn400 and
AK	RND		469.7 km	28.0 deg	Streckeisen STS-2 G3/Quanterra 330 Linear Phase
AK	SGA		456.1 km	75.5 deg	Nanometrics Trillium 240 Sec Response sn400 and
AK	SII		359.4 km	189.0 deg	Nanometrics Trillium 240 Sec Response sn400 and
AK	SUCK		531.8 km	82.0 deg	Nanometrics Trillium 120 Sec Response/Quanterra
AK	TRF		441.5 km	19.7 deg	Streckeisen STS-2 G3/Quanterra 330 Linear Phase
AK	VRDI		563.5 km	68.8 deg	Nanometrics Trillium 240 Sec Response sn400 and
AK	WAX		584.1 km	77.9 deg	Nanometrics Trillium 120 Sec Response/Quanterra
AK	WRH		591.1 km	24.9 deg	Nanometrics Trillium 240 Sec Response sn400 and
--					
AK	MCK		499.1 km	25.4 deg	Nanometrics Trillium 120 Sec Response/Quanterra
AK	PAX		549.7 km	45.9 deg	Nanometrics Trillium 120 Sec Response/Quanterra
AK	NEA2		582.1 km	20.2 deg	Nanometrics Trillium 120 Sec Response/Quanterra
AK	HDA		614.8 km	29.7 deg	Nanometrics Trillium 120 Sec Response/Quanterra
AK	RIDG		628.2 km	41.4 deg	Nanometrics Trillium 120 Sec Response/Quanterra
AK	MDM		636.1 km	22.0 deg	Nanometrics Trillium 120 Sec Response/Quanterra
AK	DOT		651.4 km	44.3 deg	Nanometrics Trillium 120 Sec Response/Quanterra
AK	SCRK		677.3 km	42.0 deg	Nanometrics Trillium 120 Sec Response/Quanterra
AT	MENT		621.5 km	51.1 deg	Trillium-240/Trident
AT	MID		393.0 km	92.2 deg	STS-2/Trident
AT	OHAK		281.5 km	180.2 deg	STS-2/Trident
AT	PMR		305.4 km	46.0 deg	STS-2/Trident
CN	BVCY		731.0 km	60.7 deg	Guralp CMG3ESP_NSN/Taurus Standard 47k
CN	YUK2		712.5 km	66.3 deg	Guralp CMG3ESP_60sec/Taurus Standard 47k
CN	YUK3		732.5 km	66.6 deg	Guralp CMG3ESP_60sec/Taurus Standard 47k
II	KDAK	10	222.7 km	169.4 deg	Nanometrics Trillium 120Posthole BB Seismometer
IU	COLA	00	635.7 km	23.8 deg	Geotech KS-54000Borehole Seismometer
IU	COLA	10	635.7 km	23.8 deg	Streckeisen STS-2 High-gain
IU	COLA	10	635.7 km	23.8 deg	Streckeisen STS-2 High-gain
PS	PS07		670.4 km	20.3 deg	cmg3esp_30sec+q330_lb100c@50
PS	PS08		630.4 km	29.4 deg	cmg3esp_60sec+q330_lb100c@50
TA	H24K		731.5 km	19.7 deg	Streckeisen STS-5A/Quanterra 330 Linear Phase Co
TA	I23K		634.3 km	16.8 deg	Streckeisen STS-5A/Quanterra 330 Linear Phase Co
TA	L26K		642.7 km	51.2 deg	Nanometrics Trillium 120 Sec Response/Quanterra
TA	L27K		712.5 km	53.9 deg	Streckeisen STS-5A/Quanterra 330 Linear Phase Co
TA	M26K		627.4 km	57.5 deg	Streckeisen STS-5A/Quanterra 330 Linear Phase Co
TA	M27K		679.3 km	59.8 deg	Nanometrics Trillium 120 Sec Response/Quanterra
TA	N19K		136.2 km	331.0 deg	Nanometrics Trillium 120 Sec Response/Quanterra
TA	N25K		516.6 km	62.7 deg	Nanometrics Trillium 120 Sec Response/Quanterra
TA	O18K		109.4 km	276.9 deg	Nanometrics Trillium 120 Sec Response/Quanterra
TA	O19K		76.8 km	310.7 deg	Nanometrics Trillium 120 Sec Response/Quanterra
TA	P18K		117.7 km	251.0 deg	Nanometrics Trillium 120 Sec Response/Quanterra
TA	POKR		669.2 km	24.2 deg	Nanometrics Trillium 240 Sec Response sn400 and
TA	POKR	01	669.2 km	24.2 deg	Streckeisen STS-4B/Quanterra 330 Linear Phase Co
TA	Q23K		392.9 km	92.2 deg	Nanometrics Trillium 120 Sec Response/Quanterra
TA	TCOL		635.7 km	23.8 deg	Streckeisen STS-4B/Quanterra 330 Linear Phase Co
XV	F1TN		586.7 km	19.6 deg	Nanometrics Trillium 120 Sec PH Response/Quanter
XV	F2TN		592.8 km	19.5 deg	Nanometrics Trillium 120 Sec PH Response/Quanter
XV	F3TN		598.9 km	19.1 deg	Nanometrics Trillium 120 Sec PH Response/Quanter
XV	F4TN		605.2 km	18.9 deg	Nanometrics Trillium 120 Sec PH Response/Quanter
XV	F5MN		610.1 km	18.5 deg	Nanometrics Trillium 120 Sec PH Response/Quanter
XV	F6TP		601.9 km	17.0 deg	Nanometrics Trillium 120 Sec PH Response/Quanter
XV	F7TV		596.0 km	15.9 deg	Nanometrics Trillium 120 Sec PH Response/Quanter
XV	F8KN		585.1 km	15.8 deg	Nanometrics Trillium 120 Sec PH Response/Quanter
XV	FAPT		577.5 km	20.4 deg	Nanometrics Trillium 120 Sec PH Response/Quanter
XV	FNN1		577.1 km	19.7 deg	Nanometrics Trillium 120 Sec PH Response/Quanter
XV	FNN2		573.3 km	18.7 deg	Nanometrics Trillium 120 Sec PH Response/Quanter
XV	FPAP		583.6 km	20.0 deg	Nanometrics Trillium 120 Sec PH Response/Quanter
XV	FTGH		596.9 km	20.8 deg	Nanometrics Trillium 120 Sec PH Response/Quanter
ZE	HLC3		94.8 km	359.8 deg	Nanometrics Trillium 120 Sec PH Response/Quanter
ZE	HLC5		118.2 km	339.4 deg	Nanometrics Trillium 120 Sec PH Response/Quanter
ZE	WFLS		152.9 km	328.2 deg	Nanometrics Trillium 120 Sec PH Response/Quanter

Table 4: 60 stations with "bad" seismograms for the M_w 7.1 Iniskin earthquake. The list is sorted by epicentral distance: 40 are <250 km, 20 are ≥250 km. These seismograms are shown in Figure 9.

net	sta	loc	distance	azimuth	response_file
AV	AU22		42.6 km	186.7 deg	CMG-6TD
AV	AUSS		44.5 km	191.9 deg	CMG-6TD
AV	AUWS		44.9 km	194.0 deg	CMG-6TD
AV	AUJA		46.5 km	190.8 deg	CMG-6TD
AV	AUSB		47.3 km	191.0 deg	CMG-6TD
TA	O20K		51.7 km	44.1 deg	Streckeisen STS-5A/Quanterra 330 Linear Phase Co
AV	RED		79.5 km	20.1 deg	CMG-6TD
AK	HOM		91.7 km	95.8 deg	Streckeisen STS-5/Quanterra 330Linear Phase Bel
AV	NCT		92.4 km	11.7 deg	CMG-6TD
TA	Q19K		93.9 km	193.3 deg	Streckeisen STS-5A/Quanterra 330 Linear Phase Co
ZE	KALS		95.2 km	43.9 deg	Nanometrics Trillium 120 Sec PH Response/Quanter
ZE	NNIL		96.6 km	69.2 deg	Nanometrics Trillium 120 Sec PH Response/Quanter
AV	RDDF		99.1 km	18.8 deg	CMG-6TD
ZE	KALN		113.6 km	42.0 deg	Nanometrics Trillium 120 Sec PH Response/Quanter
AK	CNP		117.4 km	101.4 deg	Nanometrics Trillium 240 Sec Response sn400 and
ZE	CLAM		118.0 km	61.8 deg	Nanometrics Trillium 120 Sec PH Response/Quanter
ZE	LTUY		131.3 km	65.5 deg	Nanometrics Trillium 120 Sec PH Response/Quanter
AK	BRLK		132.9 km	88.9 deg	Streckeisen STS-2 G3/Quanterra 330 Linear Phase
ZE	SALA		140.1 km	37.3 deg	Nanometrics Trillium 120 Sec PH Response/Quanter
ZE	LTUX		140.8 km	70.1 deg	Nanometrics Trillium 120 Sec PH Response/Quanter
AK	BRSE		142.2 km	89.3 deg	Nanometrics Trillium 240 Sec Response sn400 and
ZE	SOLD		145.4 km	55.9 deg	Nanometrics Trillium 120 Sec PH Response/Quanter
ZE	NSKI		150.1 km	46.5 deg	Nanometrics Trillium 120 Sec PH Response/Quanter
AK	CAPN		163.1 km	45.0 deg	Nanometrics Trillium 120 Sec Response/Quanterra
ZE	BING		166.2 km	58.0 deg	Nanometrics Trillium 120 Sec PH Response/Quanter
AV	SPCR		171.8 km	19.4 deg	CMG-6TD
ZE	CONG		179.0 km	34.6 deg	Nanometrics Trillium 120 Sec PH Response/Quanter
AV	SPCG		184.9 km	21.2 deg	CMG-6TD
AK	SLK		189.4 km	62.1 deg	Nanometrics Trillium 240 Sec Response sn400 and
ZE	MPEN		189.4 km	53.4 deg	Nanometrics Trillium 120 Sec PH Response/Quanter
AV	KAKN		191.9 km	213.2 deg	CMG-6TD
ZE	WHIP		198.8 km	45.9 deg	Nanometrics Trillium 120 Sec PH Response/Quanter
AV	KABU		201.4 km	215.9 deg	CMG-6TD
TA	O22K		213.3 km	66.0 deg	Nanometrics Trillium 120 Sec Response/Quanterra
AK	SWD		217.1 km	77.9 deg	Guralp CMG3ESP_60sec/Quanterra 330 Linear Phase
II	KDAK	00	222.7 km	169.4 deg	Geotech KS-54000Borehole Seismometer
ZE	JUDD		223.2 km	24.2 deg	Nanometrics Trillium 120 Sec PH Response/Quanter
AK	FIRE		228.7 km	46.0 deg	Nanometrics Trillium 120 Sec Response/Quanterra
ZE	HOPE		238.5 km	56.8 deg	Nanometrics Trillium 120 Sec PH Response/Quanter
AK	RC01		245.1 km	51.0 deg	Nanometrics Trillium 120 Sec Response/Quanterra
ZE	GOOS		261.9 km	44.2 deg	Nanometrics Trillium 120 Sec PH Response/Quanter
TA	M22K		281.6 km	36.2 deg	Streckeisen STS-4B/Quanterra 330 Linear Phase Co
AK	PWL		299.5 km	63.5 deg	Nanometrics Trillium 120 Sec Response/Quanterra
AK	KNK		322.2 km	52.8 deg	Nanometrics Trillium 120 Sec Response/Quanterra
AK	GHO		326.7 km	44.6 deg	Nanometrics Trillium 120 Sec Response/Quanterra
AK	CUT		337.5 km	27.4 deg	Nanometrics Trillium 120 Sec Response/Quanterra
AK	SAW		353.3 km	47.4 deg	Nanometrics Trillium 120 Sec Response/Quanterra
AK	GLI		363.5 km	67.1 deg	Nanometrics Trillium 120 Sec Response/Quanterra
AK	FID		385.1 km	70.7 deg	Nanometrics Trillium 240 Sec Response sn400 and
AK	SCM		397.9 km	51.8 deg	Nanometrics Trillium 240 Sec Response sn400 and
PS	VMT		408.0 km	65.7 deg	cmg3esp_60sec+q330_lb100c@50
AK	DIV		440.0 km	66.3 deg	Nanometrics Trillium 120 Sec Response/Quanterra
AK	KLU		446.3 km	61.1 deg	Nanometrics Trillium 240 Sec Response sn400 and
TA	M24K		465.4 km	52.6 deg	Nanometrics Trillium 120 Sec Response/Quanterra
PS	PS12		484.2 km	63.1 deg	cmg3esp_60sec+q330_lb100c@50
PS	PS11		495.7 km	55.1 deg	cmg3esp_60sec+q330_lb100c@50
TA	HARP		527.5 km	52.5 deg	Streckeisen STS-4B/Quanterra 330 Linear Phase Co
AK	BGLC		559.3 km	81.5 deg	Nanometrics Trillium 120 Sec Response/Quanterra
PS	PS10		570.5 km	41.0 deg	cmg3t_100sec+q330_lb100c@50
PS	PS09		610.0 km	37.0 deg	cmg3esp_60sec+q330_lb100c@50

Table 5: Same as Table 4, but here the stations are grouped by network. The lower set of AK stations are posthole sensors (HOM, CAPN, RC01, KNK, CUT, SAW).

net	sta	loc	distance	azimuth	response_file
AK	SCM		397.9 km	51.8 deg	Nanometrics Trillium 240 Sec Response sn400 and
AK	GLI		363.5 km	67.1 deg	Nanometrics Trillium 120 Sec Response/Quanterra
AK	FID		385.1 km	70.7 deg	Nanometrics Trillium 240 Sec Response sn400 and
AK	BGLC		559.3 km	81.5 deg	Nanometrics Trillium 120 Sec Response/Quanterra
AK	BRSE		142.2 km	89.3 deg	Nanometrics Trillium 240 Sec Response sn400 and
AK	KLU		446.3 km	61.1 deg	Nanometrics Trillium 240 Sec Response sn400 and
AK	GHO		326.7 km	44.6 deg	Nanometrics Trillium 120 Sec Response/Quanterra
AK	PWL		299.5 km	63.5 deg	Nanometrics Trillium 120 Sec Response/Quanterra
AK	SLK		189.4 km	62.1 deg	Nanometrics Trillium 240 Sec Response sn400 and
AK	CNP		117.4 km	101.4 deg	Nanometrics Trillium 240 Sec Response sn400 and
AK	BRLK		132.9 km	88.9 deg	Streckeisen STS-2 G3/Quanterra 330 Linear Phase
AK	SWD		217.1 km	77.9 deg	Guralp CMG3ESP_60sec/Quanterra 330 Linear Phase
AK	FIRE		228.7 km	46.0 deg	Nanometrics Trillium 120 Sec Response/Quanterra
AK	DIV		440.0 km	66.3 deg	Nanometrics Trillium 120 Sec Response/Quanterra
--					
AK	HOM		91.7 km	95.8 deg	Streckeisen STS-5/Quanterra 330Linear Phase Bel
AK	CAPN		163.1 km	45.0 deg	Nanometrics Trillium 120 Sec Response/Quanterra
AK	RC01		245.1 km	51.0 deg	Nanometrics Trillium 120 Sec Response/Quanterra
AK	KNK		322.2 km	52.8 deg	Nanometrics Trillium 120 Sec Response/Quanterra
AK	CUT		337.5 km	27.4 deg	Nanometrics Trillium 120 Sec Response/Quanterra
AK	SAW		353.3 km	47.4 deg	Nanometrics Trillium 120 Sec Response/Quanterra
AV	NCT		92.4 km	11.7 deg	CMG-6TD
AV	RDDF		99.1 km	18.8 deg	CMG-6TD
AV	RED		79.5 km	20.1 deg	CMG-6TD
AV	SPCR		171.8 km	19.4 deg	CMG-6TD
AV	SPCG		184.9 km	21.2 deg	CMG-6TD
AV	KAKN		191.9 km	213.2 deg	CMG-6TD
AV	AUSB		47.3 km	191.0 deg	CMG-6TD
AV	AUWS		44.9 km	194.0 deg	CMG-6TD
AV	AUSS		44.5 km	191.9 deg	CMG-6TD
AV	AU22		42.6 km	186.7 deg	CMG-6TD
AV	KABU		201.4 km	215.9 deg	CMG-6TD
AV	AUJA		46.5 km	190.8 deg	CMG-6TD
II	KDAK	00	222.7 km	169.4 deg	Geotech KS-54000Borehole Seismometer
PS	PS09		610.0 km	37.0 deg	cmg3esp_60sec+q330_lb100c@50
PS	PS10		570.5 km	41.0 deg	cmg3t_100sec+q330_lb100c@50
PS	PS11		495.7 km	55.1 deg	cmg3esp_60sec+q330_lb100c@50
PS	PS12		484.2 km	63.1 deg	cmg3esp_60sec+q330_lb100c@50
PS	VMT		408.0 km	65.7 deg	cmg3esp_60sec+q330_lb100c@50
TA	O20K		51.7 km	44.1 deg	Streckeisen STS-5A/Quanterra 330 Linear Phase Co
TA	O22K		213.3 km	66.0 deg	Nanometrics Trillium 120 Sec Response/Quanterra
TA	HARP		527.5 km	52.5 deg	Streckeisen STS-4B/Quanterra 330 Linear Phase Co
TA	M22K		281.6 km	36.2 deg	Streckeisen STS-4B/Quanterra 330 Linear Phase Co
TA	Q19K		93.9 km	193.3 deg	Streckeisen STS-5A/Quanterra 330 Linear Phase Co
TA	M24K		465.4 km	52.6 deg	Nanometrics Trillium 120 Sec Response/Quanterra
ZE	KALS		95.2 km	43.9 deg	Nanometrics Trillium 120 Sec PH Response/Quanter
ZE	MPEN		189.4 km	53.4 deg	Nanometrics Trillium 120 Sec PH Response/Quanter
ZE	GOOS		261.9 km	44.2 deg	Nanometrics Trillium 120 Sec PH Response/Quanter
ZE	JUDD		223.2 km	24.2 deg	Nanometrics Trillium 120 Sec PH Response/Quanter
ZE	CONG		179.0 km	34.6 deg	Nanometrics Trillium 120 Sec PH Response/Quanter
ZE	SALA		140.1 km	37.3 deg	Nanometrics Trillium 120 Sec PH Response/Quanter
ZE	LTUX		140.8 km	70.1 deg	Nanometrics Trillium 120 Sec PH Response/Quanter
ZE	LTUY		131.3 km	65.5 deg	Nanometrics Trillium 120 Sec PH Response/Quanter
ZE	NNIL		96.6 km	69.2 deg	Nanometrics Trillium 120 Sec PH Response/Quanter
ZE	HOPE		238.5 km	56.8 deg	Nanometrics Trillium 120 Sec PH Response/Quanter
ZE	NSKI		150.1 km	46.5 deg	Nanometrics Trillium 120 Sec PH Response/Quanter
ZE	CLAM		118.0 km	61.8 deg	Nanometrics Trillium 120 Sec PH Response/Quanter
ZE	KALN		113.6 km	42.0 deg	Nanometrics Trillium 120 Sec PH Response/Quanter
ZE	WHIP		198.8 km	45.9 deg	Nanometrics Trillium 120 Sec PH Response/Quanter
ZE	SOLD		145.4 km	55.9 deg	Nanometrics Trillium 120 Sec PH Response/Quanter
ZE	BING		166.2 km	58.0 deg	Nanometrics Trillium 120 Sec PH Response/Quanter

Table 6: Max counts ($\max[c(t)]$) on each component for the (good) stations in Table 2. The `clipping` column is the ratio of the max counts on any of the three components to the (threshold) value $q = |2^{N-1}|$ for the N-bit digitizer. The `time steps` columns show the number of time steps for which $|c(t)| > 0.8q$. This gives an indication of the severity of clipping and the likelihood of a seismogram having squared waveforms.

net	sta	loc	channels	distance	azimuth	max counts on each component			----time steps----			clipping	sensor
TA	O19K		BHZ BHE BHN	76.8 km	310.7 deg	4993574	6219785	10102073	0	0	31	1.20 (24-bit)	Nanometrics Trillium 120 Sec Response/Quanterra
ZE	HLC3		HHZ HHE HHN	94.8 km	359.8 deg	6770713	6834158	9869933	7	6	191	1.18 (24-bit)	Nanometrics Trillium 120 Sec PH Response/Quanter
TA	O18K		BHZ BHE BHN	109.4 km	276.9 deg	1635492	2091133	5307763	0	0	0	0.63 (24-bit)	Nanometrics Trillium 120 Sec Response/Quanterra
TA	P18K		BHZ BHE BHN	117.7 km	251.0 deg	1186736	2216362	1756318	0	0	0	0.26 (24-bit)	Nanometrics Trillium 120 Sec Response/Quanterra
ZE	HLC5		HHZ HHE HHN	118.2 km	339.4 deg	3962796	5762139	9056947	0	0	76	1.08 (24-bit)	Nanometrics Trillium 120 Sec PH Response/Quanter
TA	N19K		BHZ BHE BHN	136.2 km	331.0 deg	2109816	2968921	6142548	0	0	0	0.73 (24-bit)	Nanometrics Trillium 120 Sec Response/Quanterra
ZE	WFLS		HHZ HHE HHN	152.9 km	328.2 deg	1772405	2676596	4632839	0	0	0	0.55 (24-bit)	Nanometrics Trillium 120 Sec PH Response/Quanter
II	KDAK	10	BHZ BH1 BH2	222.7 km	169.4 deg	15971086	27746142	19511192	0	6	0	0.83 (26-bit)	Nanometrics Trillium 120Posthole BB Seismometer
AT	OHAK		BHZ BHE BHN	281.5 km	180.2 deg	3037254	3259302	3731011	0	0	0	0.44 (24-bit)	STS-2/Trident
AT	PMR		BHZ BHE BHN	305.4 km	46.0 deg	8433302	8460161	8473549	30	47	98	1.01 (24-bit)	STS-2/Trident
AK	PPLA		BHZ BHE BHN	355.3 km	8.9 deg	3775269	4171901	4477089	0	0	0	0.53 (24-bit)	Nanometrics Trillium 240 Sec Response sn400 and
AK	SII		BHZ BHE BHN	359.4 km	189.0 deg	2044490	3448853	4475269	0	0	0	0.53 (24-bit)	Nanometrics Trillium 240 Sec Response sn400 and
TA	Q23K		BHZ BHE BHN	392.9 km	92.2 deg	2836806	3356220	3338121	0	0	0	0.40 (24-bit)	Nanometrics Trillium 120 Sec Response/Quanterra
AT	MID		BHZ BHE BHN	393.0 km	92.2 deg	3377971	4136842	4501946	0	0	0	0.54 (24-bit)	STS-2/Trident
AK	CAST		BHZ BHE BHN	413.6 km	8.2 deg	1264864	2430307	1429290	0	0	0	0.29 (24-bit)	Nanometrics Trillium 240 Sec Response sn400 and
AK	EYAK		BHZ BHE BHN	426.8 km	74.7 deg	3876699	3968494	5500256	0	0	0	0.66 (24-bit)	Guralp CMG3T_120sec/Quanterra 330 LinearPhase B
AK	TRF		BHZ BHE BHN	441.5 km	19.7 deg	5270057	6116956	4377454	0	0	0	0.73 (24-bit)	Streckeisen STS-2 G3/Quanterra 330 Linear Phase
AK	KTH		BHZ BHE BHN	441.6 km	15.3 deg	2287505	2986624	3501217	0	0	0	0.42 (24-bit)	Nanometrics Trillium 240 Sec Response sn400 and
AK	SGA		BHZ BHE BHN	456.1 km	75.5 deg	2525113	5085220	6298988	0	0	0	0.75 (24-bit)	Nanometrics Trillium 240 Sec Response sn400 and
AK	CHI		BHZ BHE BHN	459.3 km	198.7 deg	1031582	1394809	1418865	0	0	0	0.17 (24-bit)	Nanometrics Trillium 240 Sec Response sn400 and
AK	RND		BHZ BHE BHN	469.7 km	28.0 deg	4433759	2830540	3094051	0	0	0	0.53 (24-bit)	Streckeisen STS-2 G3/Quanterra 330 Linear Phase
AK	GOAT		BHZ BHE BHN	482.8 km	75.3 deg	4037178	9736210	9727398	0	17	11	1.16 (24-bit)	Nanometrics Trillium 240 Sec Response sn400 and
AK	KAI		BHZ BHE BHN	496.3 km	83.9 deg	2749088	3513020	5649767	0	0	0	0.67 (24-bit)	Nanometrics Trillium 120 Sec Response/Quanterra
AK	BMR		BHZ BHE BHN	496.7 km	70.4 deg	4192940	3416974	5840455	0	0	0	0.70 (24-bit)	Nanometrics Trillium 120 Sec Response/Quanterra
AK	MCK		BHZ BHE BHN	499.1 km	25.4 deg	2643573	3205368	2709552	0	0	0	0.38 (24-bit)	Nanometrics Trillium 120 Sec Response/Quanterra
AK	BPAW		BHZ BHE BHN	499.3 km	12.9 deg	1207542	2297163	1133343	0	0	0	0.27 (24-bit)	Nanometrics Trillium 240 Sec Response sn400 and
AK	HMT		BHZ BHE BHN	505.8 km	78.7 deg	2248984	7906942	6729974	0	21	1	0.94 (24-bit)	Nanometrics Trillium 120 Sec Response/Quanterra
TA	N25K		BHZ BHE BHN	516.6 km	62.7 deg	3696714	3390588	4871282	0	0	0	0.58 (24-bit)	Nanometrics Trillium 120 Sec Response/Quanterra
AK	NICH		BHZ BHE BHN	521.5 km	80.0 deg	2268306	4181035	4799679	0	0	0	0.57 (24-bit)	Nanometrics Trillium 240 Sec Response sn400 and
AK	SUCK		BHZ BHE BHN	531.8 km	82.0 deg	2206736	2263843	3268650	0	0	0	0.39 (24-bit)	Nanometrics Trillium 120 Sec Response/Quanterra
AK	BWN		BHZ BHE BHN	534.9 km	21.2 deg	3672731	5470964	4752436	0	0	0	0.65 (24-bit)	Nanometrics Trillium 120 Sec Response/Quanterra
AK	BERG		BHZ BHE BHN	537.1 km	78.2 deg	2396626	6073786	4348460	0	0	0	0.72 (24-bit)	Nanometrics Trillium 240 Sec Response sn400 and
AK	PAX		BHZ BHE BHN	549.7 km	45.9 deg	2314198	3127233	3501598	0	0	0	0.42 (24-bit)	Nanometrics Trillium 120 Sec Response/Quanterra
AK	GLB		BHZ BHE BHN	550.8 km	65.9 deg	3084668	2486961	4752709	0	0	0	0.57 (24-bit)	Nanometrics Trillium 240 Sec Response sn400 and
AK	GRIN		BHZ BHE BHN	557.5 km	79.6 deg	2204443	3886586	3168592	0	0	0	0.46 (24-bit)	Streckeisen STS-2 G3/Quanterra 330 Linear Phase
AK	KHIT		BHZ BHE BHN	562.2 km	77.8 deg	2441041	3803426	3691923	0	0	0	0.45 (24-bit)	Nanometrics Trillium 240 Sec Response sn400 and
AK	VRDI		BHZ BHE BHN	563.5 km	68.8 deg	2190139	2655067	4161792	0	0	0	0.50 (24-bit)	Nanometrics Trillium 240 Sec Response sn400 and
XV	FNN2		HHZ HHE HHN	573.3 km	18.7 deg	3805498	7417033	6067250	0	53	0	0.88 (24-bit)	Nanometrics Trillium 120 Sec PH Response/Quanter
XV	FNN1		HHZ HHE HHN	577.1 km	19.7 deg	3339496	4703311	5521109	0	0	0	0.66 (24-bit)	Nanometrics Trillium 120 Sec PH Response/Quanter
XV	FAPT		HHZ HHE HHN	577.5 km	20.4 deg	1486649	5487928	3783485	0	0	0	0.65 (24-bit)	Nanometrics Trillium 120 Sec PH Response/Quanter
AK	NEA2		BHZ BHE BHN	582.1 km	20.2 deg	905426	1517160	1473710	0	0	0	0.18 (24-bit)	Nanometrics Trillium 120 Sec Response/Quanterra
XV	FPAP		HHZ HHE HHN	583.6 km	20.0 deg	1435465	3435538	3128969	0	0	0	0.41 (24-bit)	Nanometrics Trillium 120 Sec PH Response/Quanter
AK	WAX		BHZ BHE BHN	584.1 km	77.9 deg	2701299	4412952	4906949	0	0	0	0.58 (24-bit)	Nanometrics Trillium 120 Sec Response/Quanterra
XV	F8KN		HHZ HHE HHN	585.1 km	15.8 deg	1029430	1380373	838729	0	0	0	0.16 (24-bit)	Nanometrics Trillium 120 Sec PH Response/Quanter
XV	F1TN		HHZ HHE HHN	586.7 km	19.6 deg	3896753	5371291	5867679	0	0	0	0.70 (24-bit)	Nanometrics Trillium 120 Sec PH Response/Quanter
AK	WRH		BHZ BHE BHN	591.1 km	24.9 deg	1299357	1649393	1443699	0	0	0	0.20 (24-bit)	Nanometrics Trillium 240 Sec Response sn400 and
XV	F2TN		HHZ HHE HHN	592.8 km	19.5 deg	4563562	5494747	6351782	0	0	0	0.76 (24-bit)	Nanometrics Trillium 120 Sec PH Response/Quanter
XV	F7TV		HHZ HHE HHN	596.0 km	15.9 deg	1097046	3461568	2364048	0	0	0	0.41 (24-bit)	Nanometrics Trillium 120 Sec PH Response/Quanter
XV	FTGH		HHZ HHE HHN	596.9 km	20.8 deg	1253579	1547706	1553871	0	0	0	0.19 (24-bit)	Nanometrics Trillium 120 Sec PH Response/Quanter
XV	F3TN		HHZ HHE HHN	598.9 km	19.1 deg	3476721	8720245	9237408	0	152	116	1.10 (24-bit)	Nanometrics Trillium 120 Sec PH Response/Quanter
XV	F6TP		HHZ HHE HHN	601.9 km	17.0 deg	2094830	3701429	3071734	0	0	0	0.44 (24-bit)	Nanometrics Trillium 120 Sec PH Response/Quanter
XV	F4TN		HHZ HHE HHN	605.2 km	18.9 deg	2794195	5226006	7638525	0	0	43	0.91 (24-bit)	Nanometrics Trillium 120 Sec PH Response/Quanter
XV	F5MN		HHZ HHE HHN	610.1 km	18.5 deg	3513370	6085425	5170715	0	0	0	0.73 (24-bit)	Nanometrics Trillium 120 Sec PH Response/Quanter
AK	PTPK		BHZ BHE BHN	614.6 km	70.3 deg	2991363	4369646	6806963	0	0	2	0.81 (24-bit)	Nanometrics Trillium 240 Sec Response sn400 and
AK	CCB		BHZ BHE BHN	614.8 km	25.1 deg	801127	913286	1084522	0	0	0	0.13 (24-bit)	Nanometrics Trillium 240 Sec Response sn400 and
AK	HDA		BHZ BHE BHN	614.8 km	29.7 deg	1369496	2255607	1982546	0	0	0	0.27 (24-bit)	Nanometrics Trillium 120 Sec Response/Quanterra
AK	KIAG		BHZ BHE BHN	615.8 km	73.1 deg	2481809	3420196	3410497	0	0	0	0.41 (24-bit)	Nanometrics Trillium 240 Sec Response sn400 and
AK	BAL		BHZ BHE BHN	618.3 km	71.9 deg	1712380	1414496	4755714	0	0	0	0.57 (24-bit)	Nanometrics Trillium 120 Sec Response/Quanterra
AT	MENT		BHZ BHE BHN	621.5 km	51.1 deg	2315762	3357072	3722823	0	0	0	0.44 (24-bit)	Trillium-240/Trident
TA	M26K		BHZ BHE BHN	627.4 km	57.5 deg	2095257	2261093	3400542	0	0	0	0.41 (24-bit)	Streckeisen STS-5A/Quanterra 330 Linear Phase Co
AK	RIDG		BHZ BHE BHN	628.2 km	41.4 deg	2809215	3982635	4403615	0	0	0	0.52 (24-bit)	Nanometrics Trillium 120 Sec Response/Quanterra
TA	I23K		BHZ BHE BHN	634.3 km	16.8 deg	1304439	1755631	1979555	0	0	0	0.24 (24-bit)	Streckeisen STS-5A/Quanterra 330 Linear Phase Co
TA	TCOL		BHZ BHE BHN	635.7 km	23.8 deg	1524284	2275821	2687469	0	0	0	0.32 (24-bit)	Streckeisen STS-4B/Quanterra 330 Linear Phase Co
IU	COLA	00	BHZ BH1 BH2	635.7 km	23.8 deg	8000617	7851908	12872183	0	0	0	0.38 (26-bit)	Geotech KS-54000Borehole Seismometer
IU	COLA	10	BHZ BH1 BH2	635.7 km	23.8 deg	41135196	41847444	41523760	1082	1840	1763	1.25 (26-bit)	Streckeisen STS-2 High-gain
IU	COLA	10	HHZ HH1 HH2	635.7 km	23.8 deg	41572436	42427368	41653472	2694	4574	4369	1.26 (26-bit)	Streckeisen STS-2 High-gain
AK	MDM		BHZ BHE BHN	636.1 km	22.0 deg	1026647	1345987	892057	0	0	0	0.16 (24-bit)	Nanometrics Trillium 120 Sec Response/Quanterra
TA	L26K		BHZ BHE BHN	642.7 km	51.2 deg	1768737	2312539	1900285	0	0	0	0.28 (24-bit)	Nanometrics Trillium 120 Sec Response/Quanterra
AK	DOT		BHZ BHE BHN	651.4 km	44.3 deg	3020518	2819958	4048787	0	0	0	0.48 (24-bit)	Nanometrics Trillium 120 Sec Response/Quanterra
AK	BARN		BHZ BHE BHN	655.3 km	72.1 deg	2108898	1749376	1680642	0	0	0	0.25 (24-bit)	Nanometrics Trillium 240 Sec Response sn400 and
TA	POKR		BHZ BHE BHN	669.2 km	24.2 deg	781187	1300282	952091	0	0	0	0.16 (24-bit)	Nanometrics Trillium 240 Sec Response sn400 and
TA	POKR	01	BHZ BHE BHN	669.2 km	24.2 deg	1004677	1639971	1255373	0	0	0	0.20 (24-bit)	Streckeisen STS-4B/Quanterra 330 Linear Phase Co
AK	SCRK		BHZ BHE BHN	677.3 km	42.0 deg	2504288	1530481	1748018	0	0	0	0.30 (24-bit)	Nanometrics Trillium 120 Sec Response/Quanterra
TA	M27K		BHZ BHE BHN	679.3 km	59.8 deg	1044502	2175968	2484399	0	0	0	0.30 (24-bit)	Nanometrics Trillium 120 Sec Response/Quanterra
CN	YUK2		HHZ HHE HHN	712.5 km	66.3 deg	934500	1464833	2179060	0	0	0	0.26 (24-bit)	Guralp CMG3ESP_60sec/Taurus Standard 47k
TA	L27K		BHZ BHE BHN	712.5 km	53.9 deg	1189842	2019600	2089744	0	0	0	0.25 (24-bit)	Streckeisen STS-5A/Quanterra 330 Linear Phase Co
CN	BVCY		HHZ HHE HHN	731.0 km	60.7 deg	1696808	2652490	2923999	0	0	0	0.35 (24-bit)	Guralp CMG3ESP_NSN/Taurus Standard 47k
TA	H24K		BHZ BHE BHN	731.5 km	19.7 deg	1156005	1430587	840363	0	0	0	0.17 (24-bit)	Streckeisen STS-5A/Quanterra 330 Linear Phase Co
CN	YUK3		HHZ HHE HHN	732.5 km	66.6 deg	861929	1079450	1669704	0	0	0	0.20 (24-bit)	Guralp CMG3ESP_60sec/Taurus Standard 47k

Table 7: Same as Table 6, but for the (bad) stations in Table 4.

net	sta	loc	channels	distance	azimuth	max counts on each component			----time steps----			clipping	sensor
AV	AU22		BHZ BHE BHN	42.6 km	186.7 deg	19323768	20315818	21108362	1805	4668	4560	2.52 (24-bit)	CMG-6TD
AV	AUSS		BHZ BHE BHN	44.5 km	191.9 deg	7933789	8182647	8235565	1209	3997	3410	0.98 (24-bit)	CMG-6TD
AV	AUWS		BHZ BHE BHN	44.9 km	194.0 deg	8230455	8124577	8717011	1252	3060	3341	1.04 (24-bit)	CMG-6TD
AV	AUJA		BHZ BHE BHN	46.5 km	190.8 deg	8923872	8867864	9137270	1070	2996	2596	1.09 (24-bit)	CMG-6TD
AV	AUSB		BHZ BHE BHN	47.3 km	191.0 deg	8476498	9451856	8909572	683	2133	1447	1.13 (24-bit)	CMG-6TD
TA	O20K		BHZ BHE BHN	51.7 km	44.1 deg	10813312	11000126	11243780	22784	22044	256	1.34 (24-bit)	Streckeisen STS-5A/Quanterra 330 Linear Phase Co
AV	RED		BHZ BHE BHN	79.5 km	20.1 deg	7880195	8102241	8533501	643	842	1043	1.02 (24-bit)	CMG-6TD
AK	HOM		BHZ BHE BHN	91.7 km	95.8 deg	10959492	11022347	11149573	508	838	1345	1.33 (24-bit)	Streckeisen STS-5/Quanterra 330Linear Phase Bel
AV	NCT		BHZ BHE BHN	92.4 km	11.7 deg	7703836	7707954	7737413	43	268	400	0.92 (24-bit)	CMG-6TD
TA	Q19K		BHZ BHE BHN	93.9 km	193.3 deg	6689711	10790829	10825120	0	515	314	1.29 (24-bit)	Streckeisen STS-5A/Quanterra 330 Linear Phase Co
ZE	KALS		HHZ HHE HHN	95.2 km	43.9 deg	9961735	9977602	10051769	13612	24834	2078	1.20 (24-bit)	Nanometrics Trillium 120 Sec PH Response/Quanter
ZE	NNIL		HHZ HHE HHN	96.6 km	69.2 deg	10054811	10167287	10160085	234	771	957	1.21 (24-bit)	Nanometrics Trillium 120 Sec PH Response/Quanter
AV	RDDF		BHZ BHE BHN	99.1 km	18.8 deg	7899034	8407030	8287098	645	947	1357	1.00 (24-bit)	CMG-6TD
ZE	KALN		HHZ HHE HHN	113.6 km	42.0 deg	9769120	10079194	9973140	297	1964	2060	1.20 (24-bit)	Nanometrics Trillium 120 Sec PH Response/Quanter
AK	CNP		BHZ BHE BHN	117.4 km	101.4 deg	9145119	10135280	10050838	11	1047	334	1.21 (24-bit)	Nanometrics Trillium 240 Sec Response sn400 and
ZE	CLAM		HHZ HHE HHN	118.0 km	61.8 deg	10279635	10251925	10221657	485	1166	2445	1.23 (24-bit)	Nanometrics Trillium 120 Sec PH Response/Quanter
ZE	LTUY		HHZ HHE HHN	131.3 km	65.5 deg	10112214	10226253	10194548	836	2593	2847	1.22 (24-bit)	Nanometrics Trillium 120 Sec PH Response/Quanter
AK	BRLK		BHZ BHE BHN	132.9 km	88.9 deg	10330658	10762575	11561941	47	124	177	1.38 (24-bit)	Streckeisen STS-2 G3/Quanterra 330 Linear Phase
ZE	SALA		HHZ HHE HHN	140.1 km	37.3 deg	9920659	9938995	9998772	488	2089	2938	1.19 (24-bit)	Nanometrics Trillium 120 Sec PH Response/Quanter
ZE	LTUX		HHZ HHE HHN	140.8 km	70.1 deg	10091564	10180096	10180324	847	1988	2464	1.21 (24-bit)	Nanometrics Trillium 120 Sec PH Response/Quanter
AK	BRSE		BHZ BHE BHN	142.2 km	89.3 deg	9967746	10088953	9826271	146	311	118	1.20 (24-bit)	Nanometrics Trillium 240 Sec Response sn400 and
ZE	SOLD		HHZ HHE HHN	145.4 km	55.9 deg	10120190	10281287	10115145	1143	2566	4347	1.23 (24-bit)	Nanometrics Trillium 120 Sec PH Response/Quanter
ZE	NSKI		HHZ HHE HHN	150.1 km	46.5 deg	10040845	10095251	10106053	1280	3479	4796	1.20 (24-bit)	Nanometrics Trillium 120 Sec PH Response/Quanter
AK	CAPN		BHZ BHE BHN	163.1 km	45.0 deg	10180374	10290691	10309986	644	2014	2169	1.23 (24-bit)	Nanometrics Trillium 120 Sec Response/Quanterra
ZE	BING		HHZ HHE HHN	166.2 km	58.0 deg	9942616	10027808	9979415	1268	2856	3664	1.20 (24-bit)	Nanometrics Trillium 120 Sec PH Response/Quanter
AV	SPCR		BHZ BHE BHN	171.8 km	19.4 deg	18090612	18888980	18548290	989	1842	1944	2.25 (24-bit)	CMG-6TD
ZE	CONG		HHZ HHE HHN	179.0 km	34.6 deg	9959691	9960502	10007680	919	3103	2800	1.19 (24-bit)	Nanometrics Trillium 120 Sec PH Response/Quanter
AV	SPCG		BHZ BHE BHN	184.9 km	21.2 deg	7711794	8170678	8118107	552	788	1370	0.97 (24-bit)	CMG-6TD
AK	SLK		BHZ BHE BHN	189.4 km	62.1 deg	9912796	10066462	10204113	210	166	612	1.22 (24-bit)	Nanometrics Trillium 240 Sec Response sn400 and
ZE	MPEN		HHZ HHE HHN	189.4 km	53.4 deg	9895881	9955874	9759976	9560	5809	12586	1.19 (24-bit)	Nanometrics Trillium 120 Sec PH Response/Quanter
AV	KAKN		BHZ BHE BHN	191.9 km	213.2 deg	1875620	1958519	1922907	0	0	0	0.23 (24-bit)	CMG-6TD
ZE	WHIP		HHZ HHE HHN	198.8 km	45.9 deg	10123953	10186301	10190664	1599	4003	4318	1.21 (24-bit)	Nanometrics Trillium 120 Sec PH Response/Quanter
AV	KABU		BHZ BHE BHN	201.4 km	215.9 deg	7691637	7780275	7705017	304	751	449	0.93 (24-bit)	CMG-6TD
TA	O22K		BHZ BHE BHN	213.3 km	66.0 deg	9979736	10133820	10204207	148	622	624	1.22 (24-bit)	Nanometrics Trillium 120 Sec Response/Quanterra
AK	SWD		BHZ BHE BHN	217.1 km	77.9 deg	7642391	7760898	7833017	812	883	1147	0.93 (24-bit)	Guralp CMG3ESP_60sec/Quanterra 330 Linear Phase
II	KDAK	00	BHZ BH1 BH2	222.7 km	169.4 deg	26335556	46992228	33462612	0	33	13	1.40 (26-bit)	Geotech KS-54000Borehole Seismometer
ZE	JUDD		HHZ HHE HHN	223.2 km	24.2 deg	10040295	10149928	10145600	288	2249	2531	1.21 (24-bit)	Nanometrics Trillium 120 Sec PH Response/Quanter
AK	FIRE		BHZ BHE BHN	228.7 km	46.0 deg	9926648	10005040	10051611	643	2138	2053	1.20 (24-bit)	Nanometrics Trillium 120 Sec Response/Quanterra
ZE	HOPE		HHZ HHE HHN	238.5 km	56.8 deg	10166516	10114685	10134948	203	294	517	1.21 (24-bit)	Nanometrics Trillium 120 Sec PH Response/Quanter
AK	RC01		BHZ BHE BHN	245.1 km	51.0 deg	9930968	9882576	10018562	463	593	210	1.19 (24-bit)	Nanometrics Trillium 120 Sec Response/Quanterra
ZE	GOOS		HHZ HHE HHN	261.9 km	44.2 deg	10036371	10284943	10099604	558	2474	2051	1.23 (24-bit)	Nanometrics Trillium 120 Sec PH Response/Quanter
TA	M22K		BHZ BHE BHN	281.6 km	36.2 deg	10302726	10379137	10273044	21185	72	55	1.24 (24-bit)	Streckeisen STS-4B/Quanterra 330 Linear Phase Co
AK	PWL		BHZ BHE BHN	299.5 km	63.5 deg	9904307	10008714	9930796	358	618	687	1.19 (24-bit)	Nanometrics Trillium 120 Sec Response/Quanterra
AK	KNK		BHZ BHE BHN	322.2 km	52.8 deg	10059242	10288186	10172936	82	262	114	1.23 (24-bit)	Nanometrics Trillium 120 Sec Response/Quanterra
AK	GHO		BHZ BHE BHN	326.7 km	44.6 deg	9794124	9809809	9791499	30	171	733	1.17 (24-bit)	Nanometrics Trillium 120 Sec Response/Quanterra
AK	CUT		BHZ BHE BHN	337.5 km	27.4 deg	7516079	9911685	9897670	33	338	370	1.18 (24-bit)	Nanometrics Trillium 120 Sec Response/Quanterra
AK	SAW		BHZ BHE BHN	353.3 km	47.4 deg	9799024	9950483	9948441	44	212	210	1.19 (24-bit)	Nanometrics Trillium 120 Sec Response/Quanterra
AK	GLI		BHZ BHE BHN	363.5 km	67.1 deg	9952728	9871144	9887031	337	42	313	1.19 (24-bit)	Nanometrics Trillium 120 Sec Response/Quanterra
AK	FID		BHZ BHE BHN	385.1 km	70.7 deg	7883288	8867035	10060070	3	42	183	1.20 (24-bit)	Nanometrics Trillium 240 Sec Response sn400 and
AK	SCM		BHZ BHE BHN	397.9 km	51.8 deg	9881385	9810633	10033545	476	536	407	1.20 (24-bit)	Nanometrics Trillium 240 Sec Response sn400 and
AK	DIV		BHZ BHE BHN	440.0 km	66.3 deg	6272481	4939321	9976108	0	0	36	1.19 (24-bit)	Nanometrics Trillium 120 Sec Response/Quanterra
AK	KLU		BHZ BHE BHN	446.3 km	61.1 deg	9801925	8587380	9881473	146	24	194	1.18 (24-bit)	Nanometrics Trillium 240 Sec Response sn400 and
TA	M24K		BHZ BHE BHN	465.4 km	52.6 deg	10024595	9991435	10022105	112	427	558	1.20 (24-bit)	Nanometrics Trillium 120 Sec Response/Quanterra
TA	HARP		BHZ BHE BHN	527.5 km	52.5 deg	10084469	10234152	10235990	7288	354	17562	1.22 (24-bit)	Streckeisen STS-4B/Quanterra 330 Linear Phase Co
AK	BGLC		BHZ BHE BHN	559.3 km	81.5 deg	5548518	9779350	8676843	0	25	24	1.17 (24-bit)	Nanometrics Trillium 120 Sec Response/Quanterra

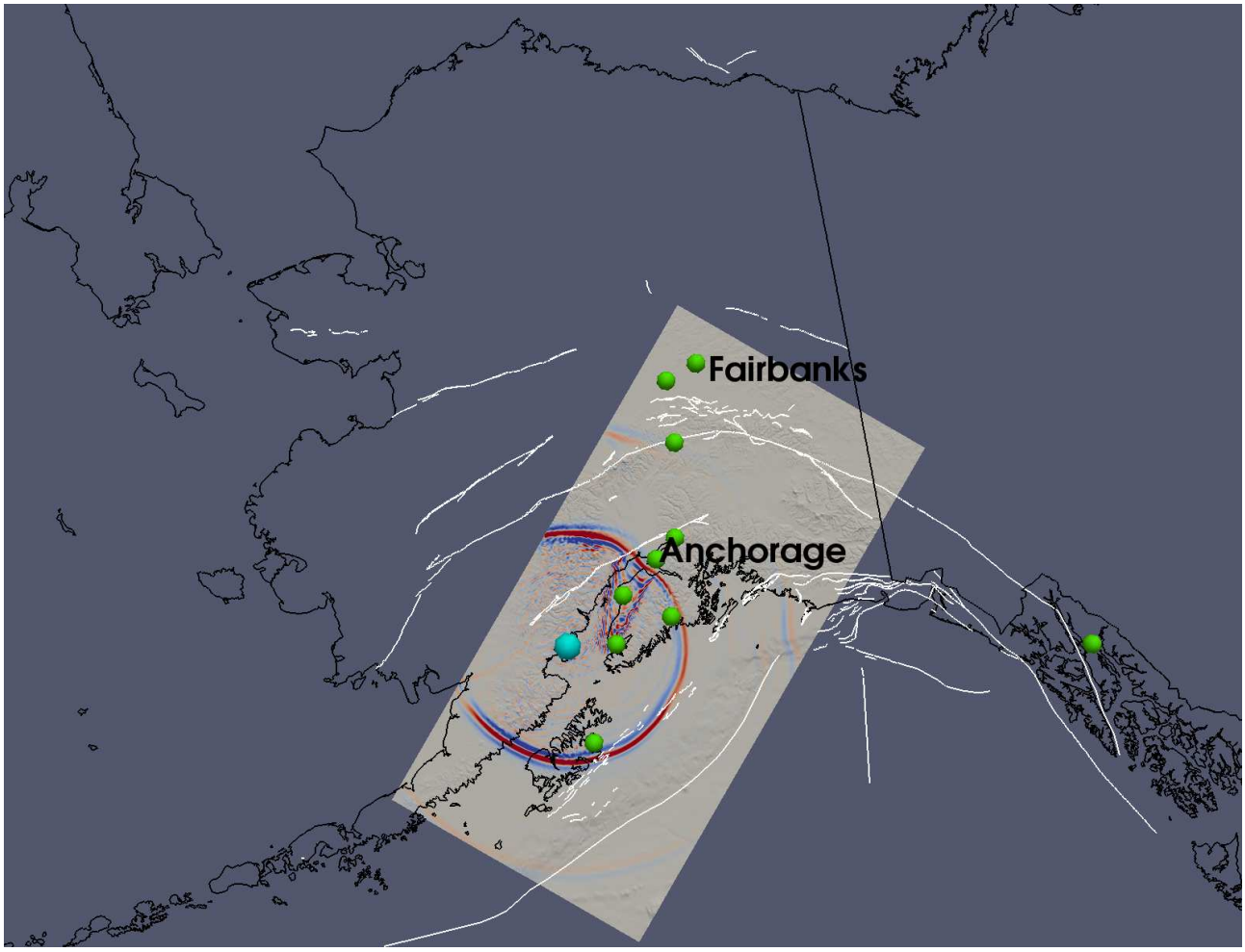

Figure 1: Map of simulation region used in this study. Only broadband stations within this 1200 km × 600 km region were analyzed. The image shows a snapshot of the wavefield simulation in *Tape* (2016a).

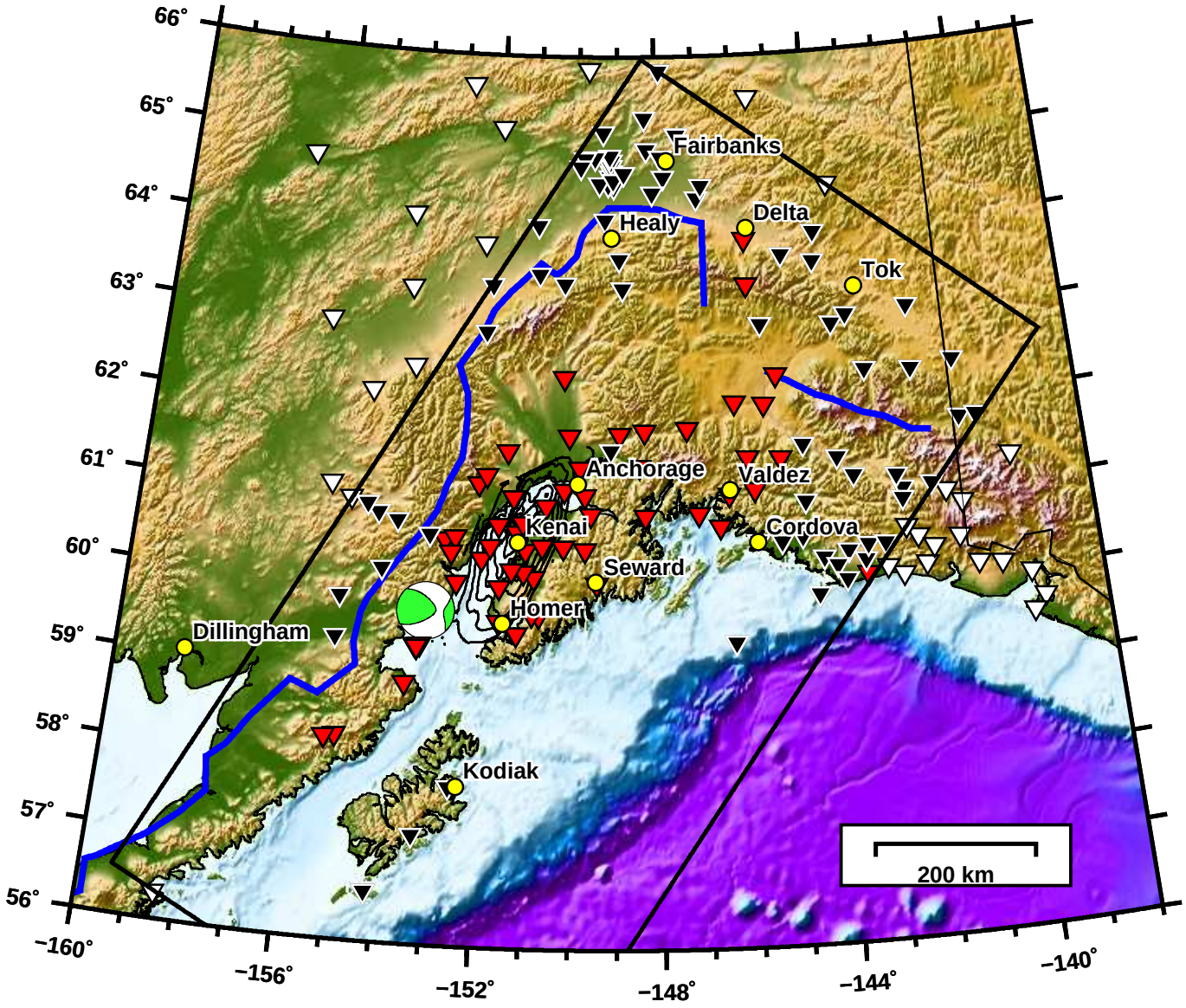

Figure 2: Map of broadband stations recording the 2016-01-24 M_w 7.1 Iniskin, Alaska, earthquake. The 1200 km × 600 km simulation region (Figure 1) is outlined in black. White: stations outside the simulation region; Black: 81 "good" stations inside the simulation region with no apparent problems; Red: 60 "bad" stations inside the simulation region. The beachball is the source mechanism from the GCMT catalog (*Ekström et al.*, 2012), which lists a depth of 111 km. The blue curve denotes the lateral extent of slab seismicity. Contours of Cook Inlet basin (*Shellenbaum et al.*, 2010) are plotted just northeast of the earthquake. See Figure 3 for a zoom-in on the Cook Inlet region.

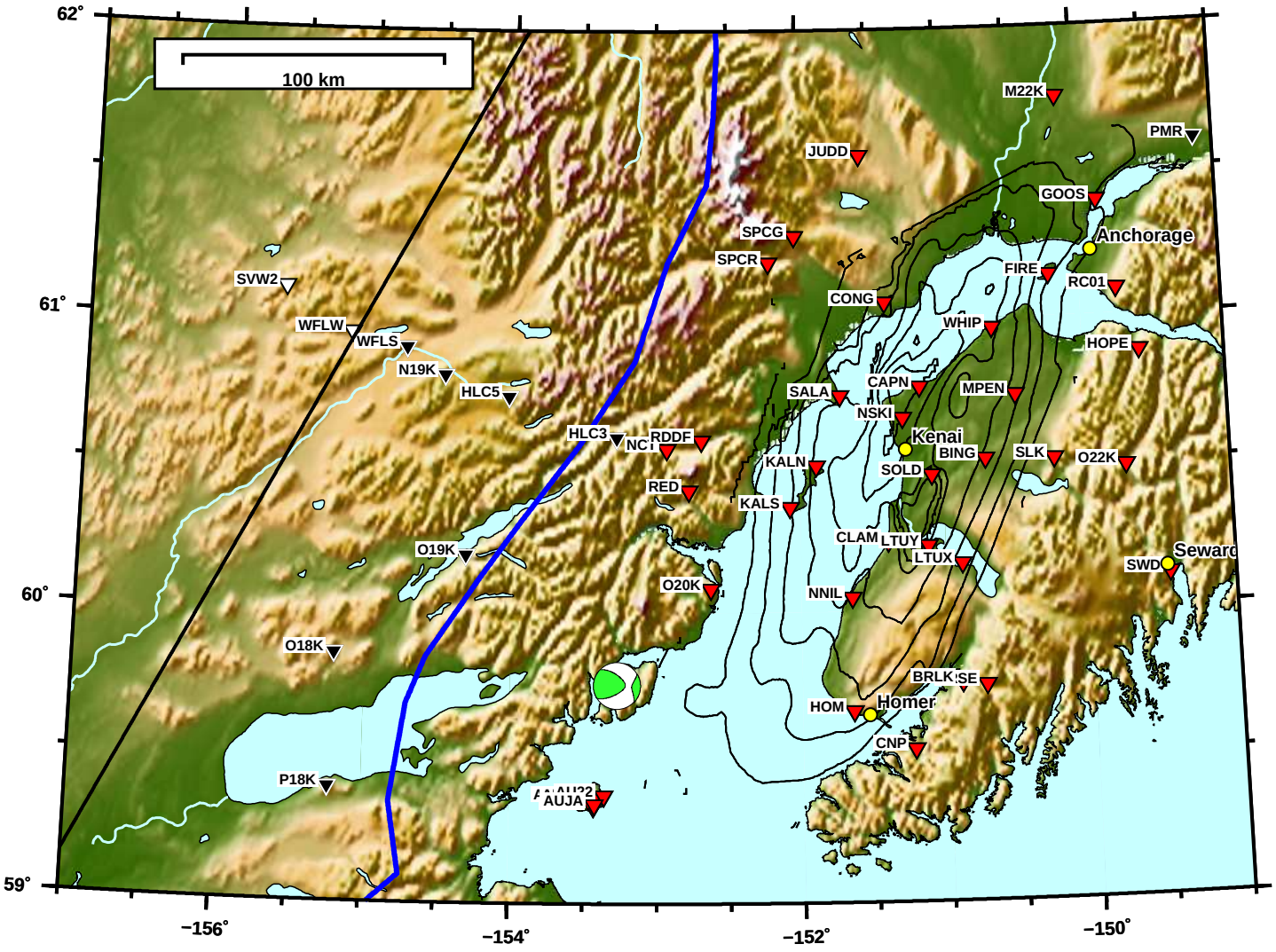

Figure 3: Zoom-in on Figure 2.

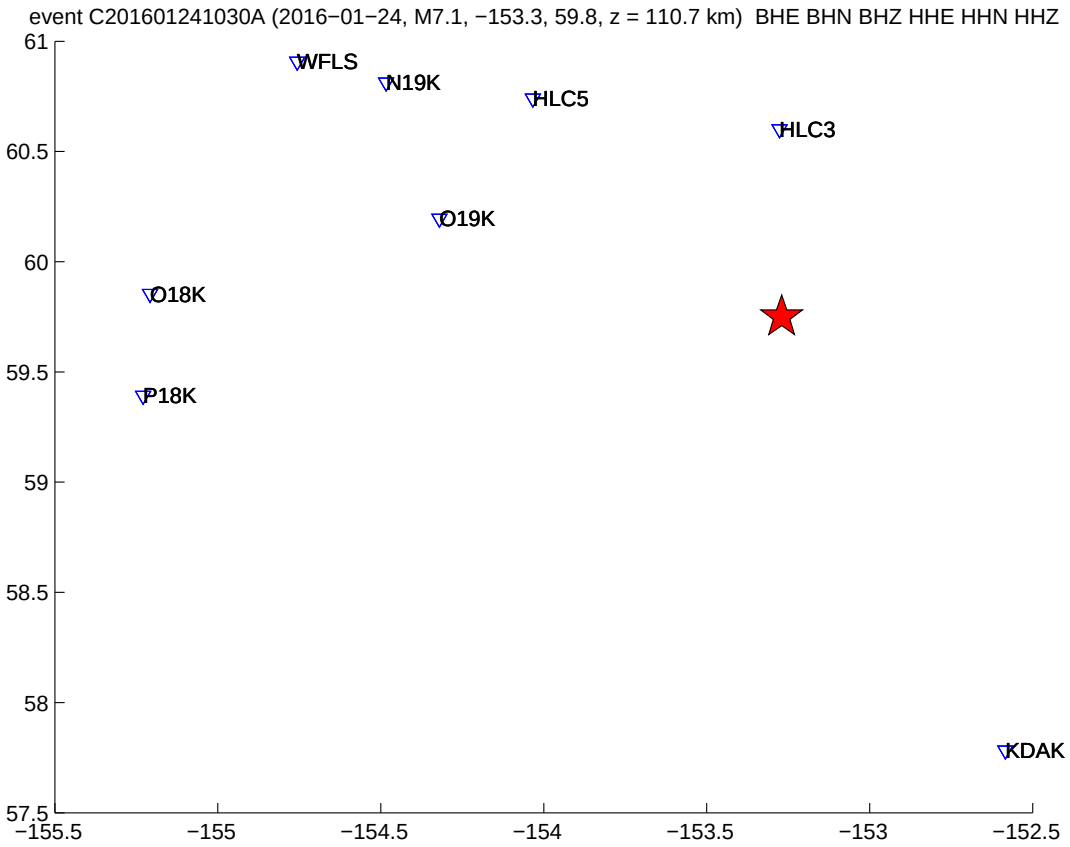

Figure 4: Map of 8 stations used in the record section in Figure 5. Note that all stations are to the northwest, whereas no station are to the northeast, where Cook Inlet basin is.

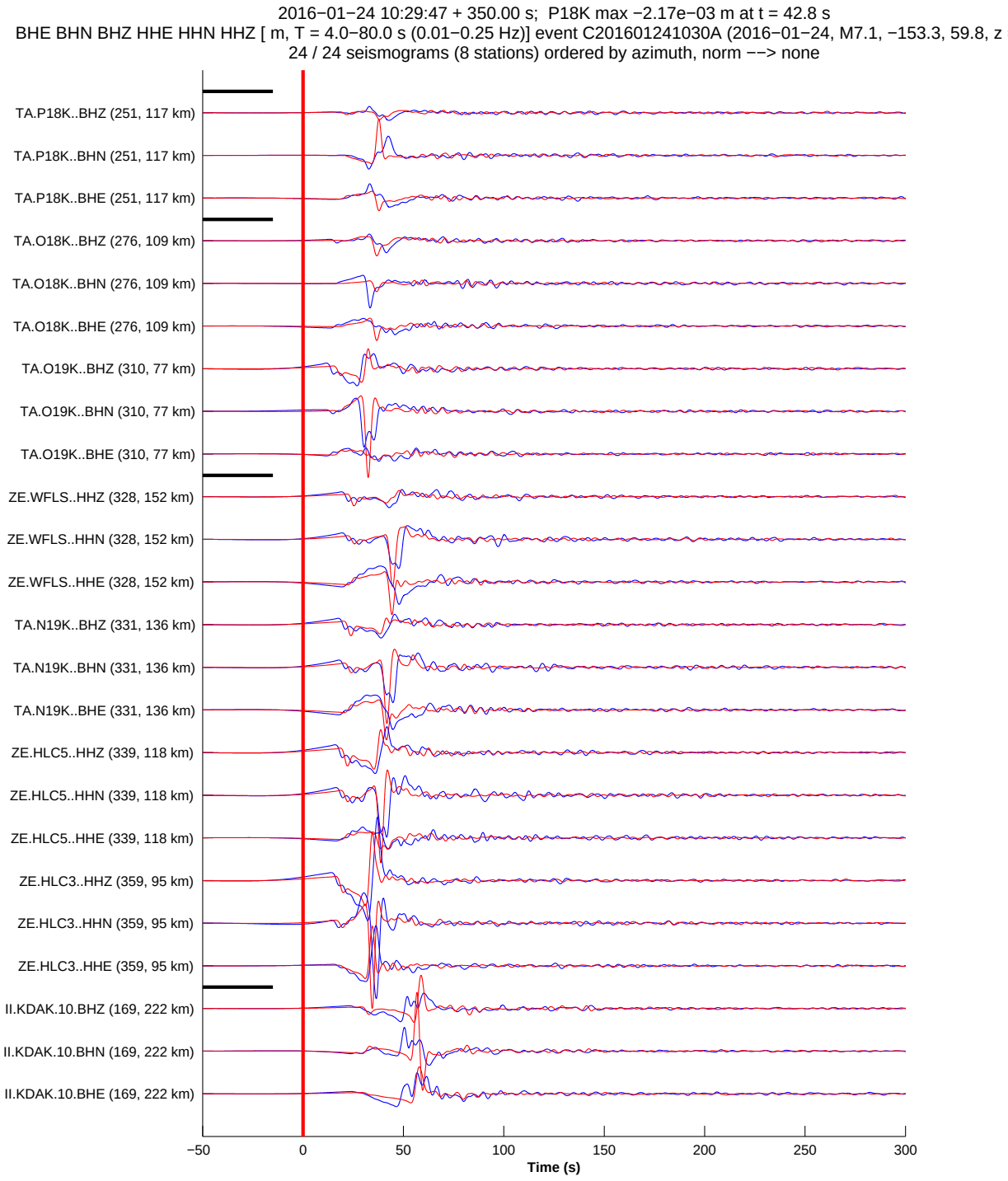

Figure 5: All 8 stations within 250 km of the Iniskin earthquake and having recorded seismograms that we deem to be good. Observed (blue) and synthetic (red) seismograms are filtered with periods 4–80 s, shown for all three components, and **sorted by station azimuth**, starting from the south. See Figure 9 for rejected stations.

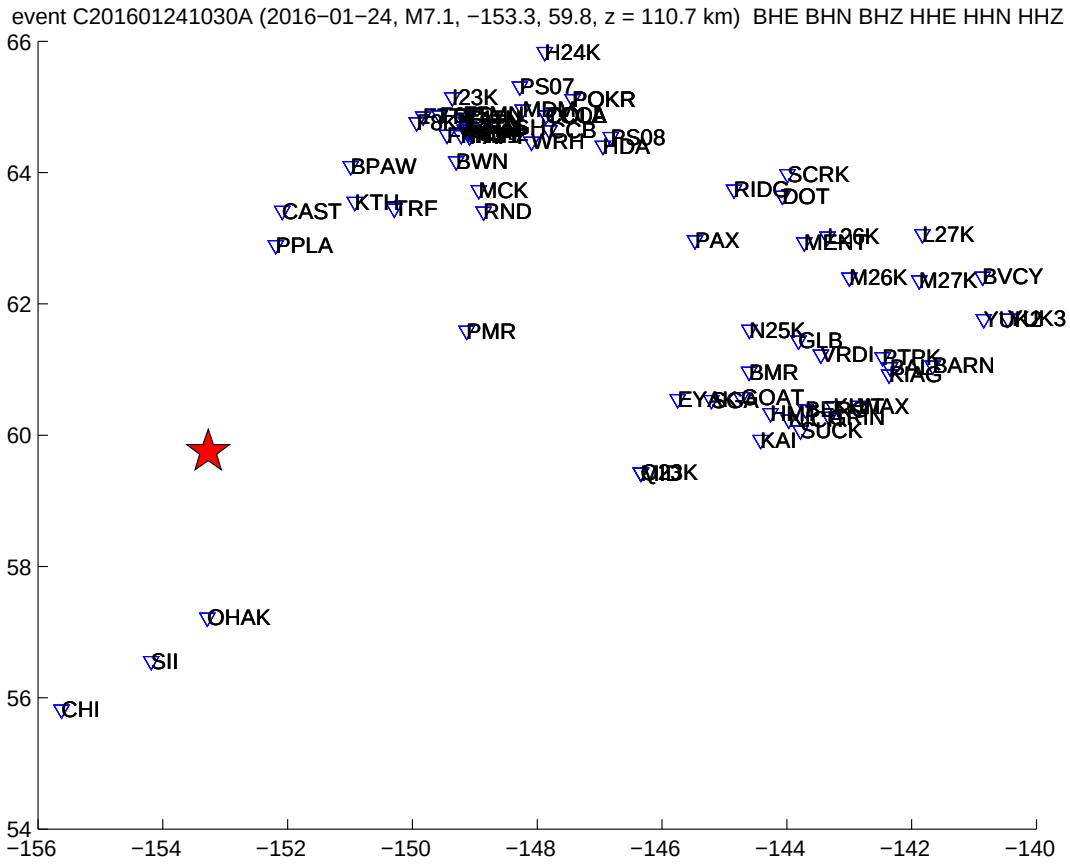

Figure 6: Map of 73 stations used in the record section in Figure 7.

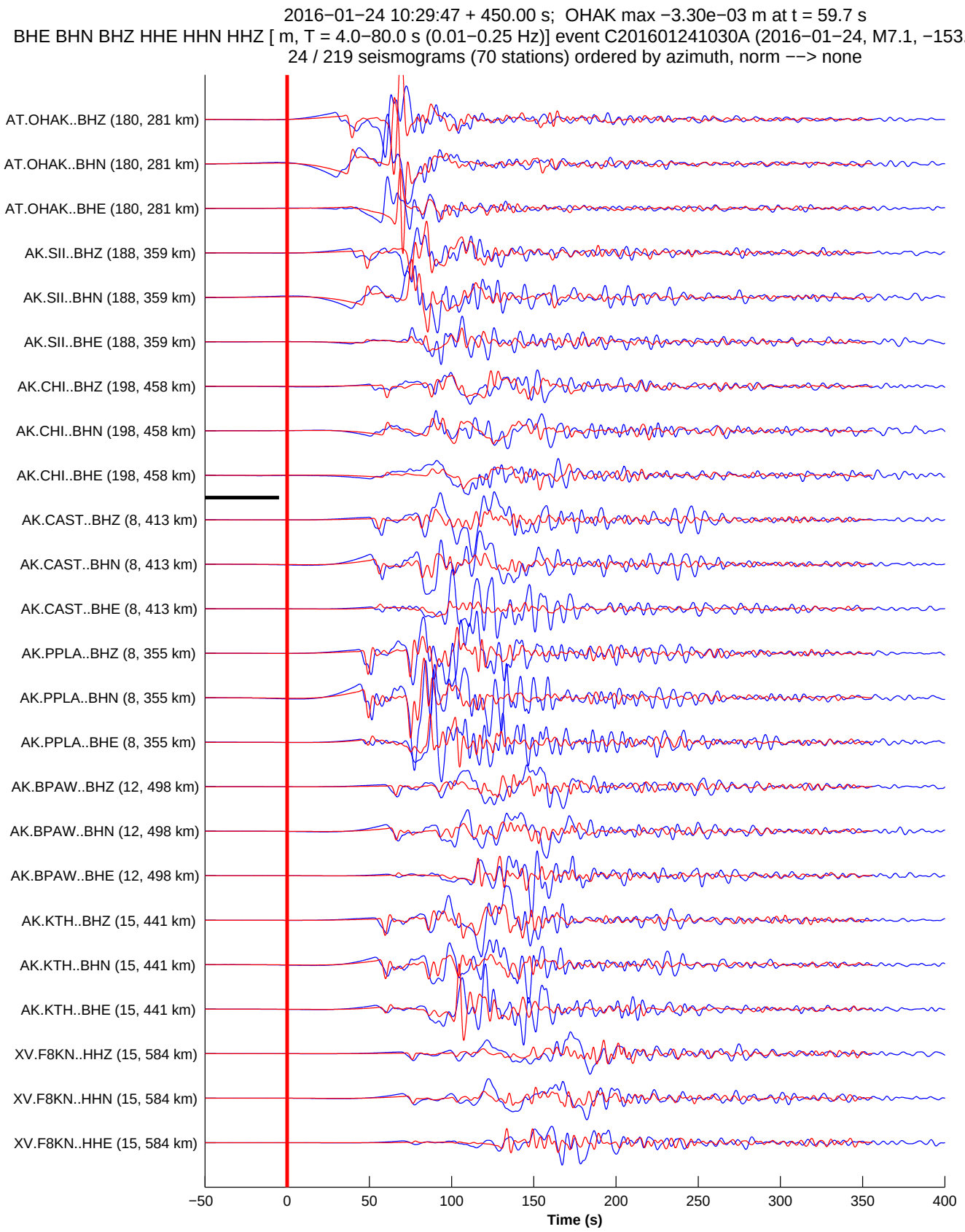

Figure 7: [CONTINUED ON FOLLOWING PAGES] All 73 stations ≥250 km of the Iniskin earthquake and having recorded seismograms that we deem to be good. No amplitude normalization (including for geometrical spreading) has been applied. Observed (blue) and synthetic (red) seismograms are filtered with periods 4–80 s, shown for all three components, and **sorted by station azimuth**, starting from the south. See Figure 9 for rejected stations.

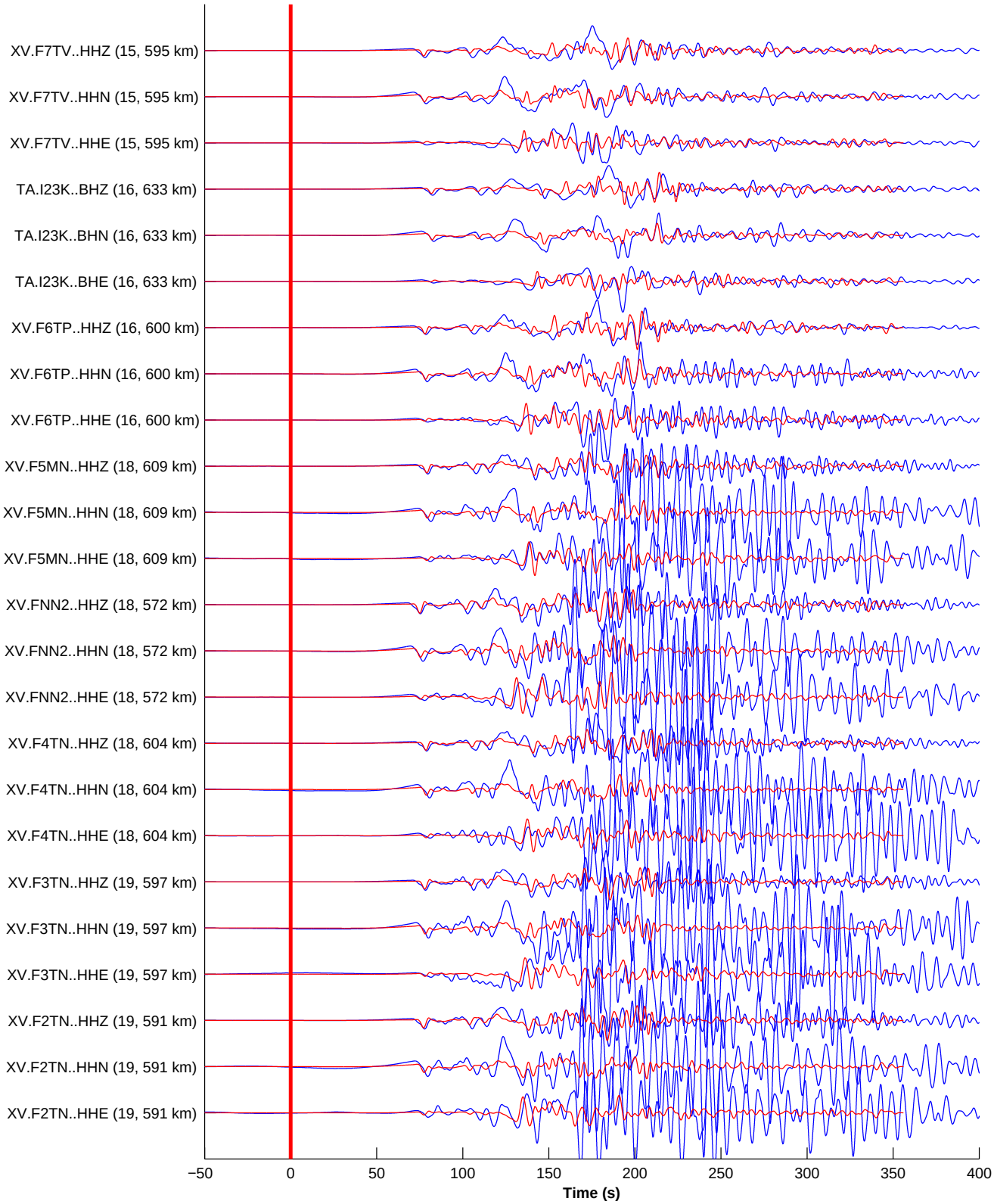

Figure 7, Part 2: station azimuths 15°–19° (FLATS/XV stations at bottom)

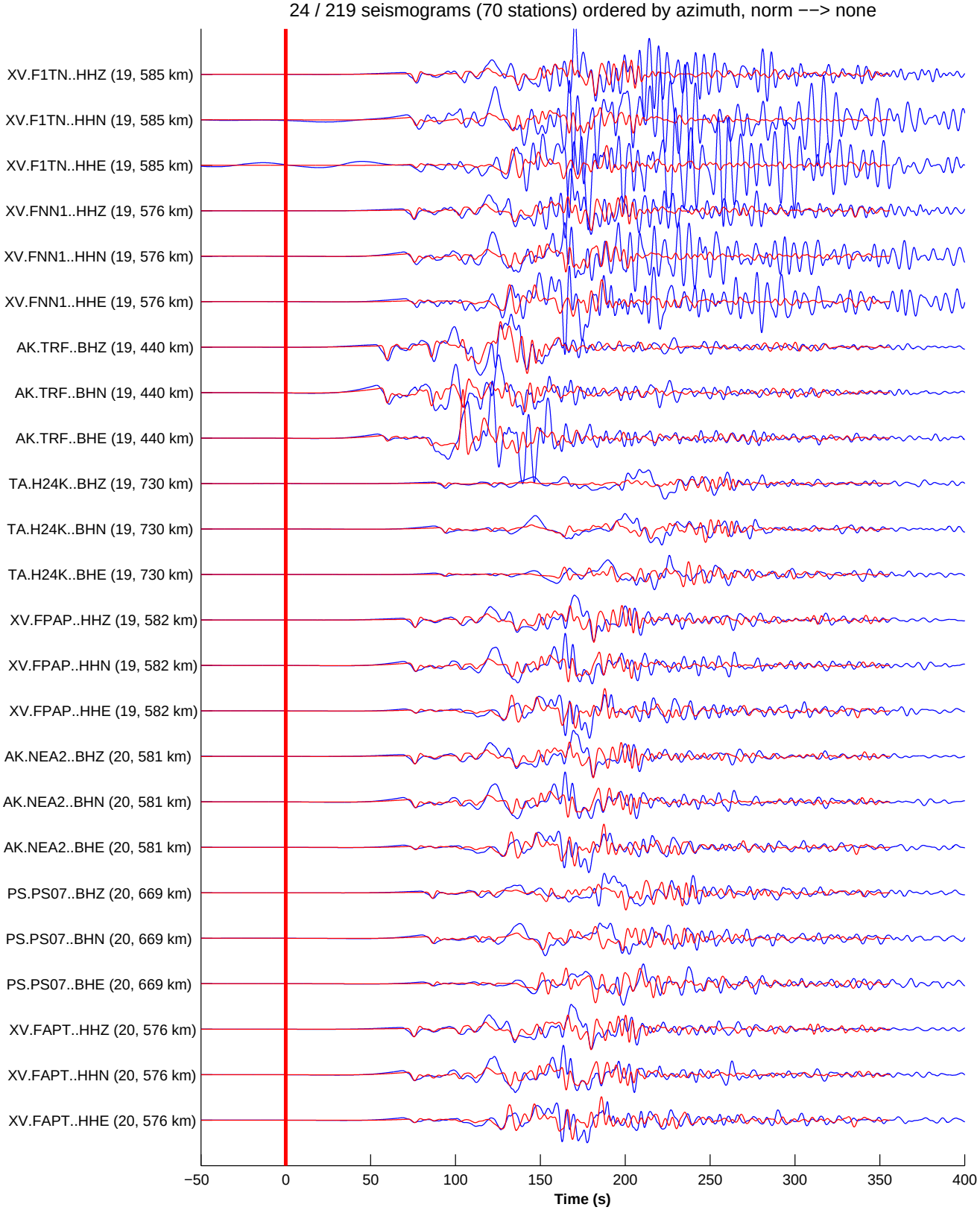

Figure 7, Part 3: station azimuths 19°–20° (FLATS/XV stations at top)

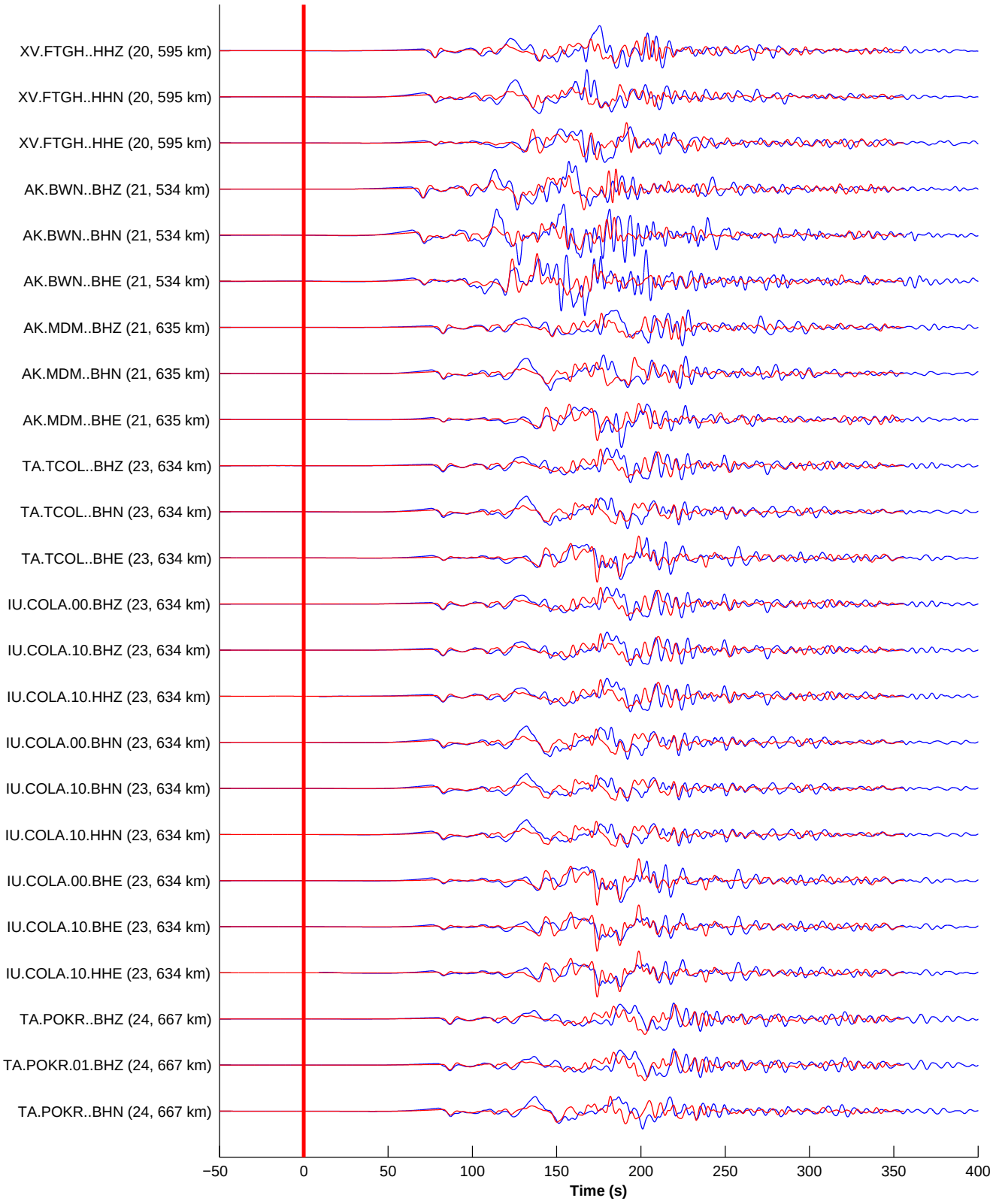

Figure 7, Part 4: station azimuths 20°–24°

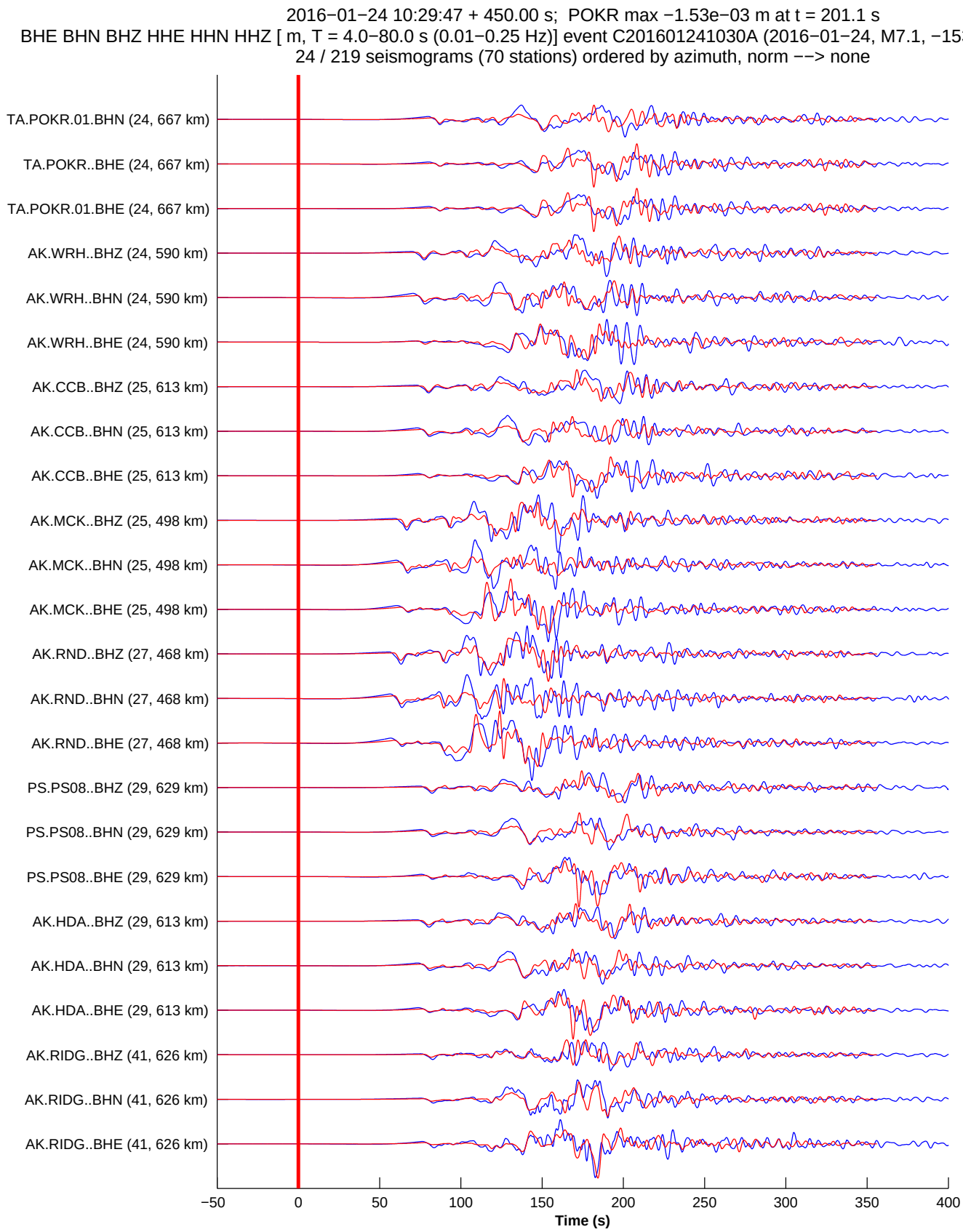

Figure 7, Part 5: station azimuths 24°–41°

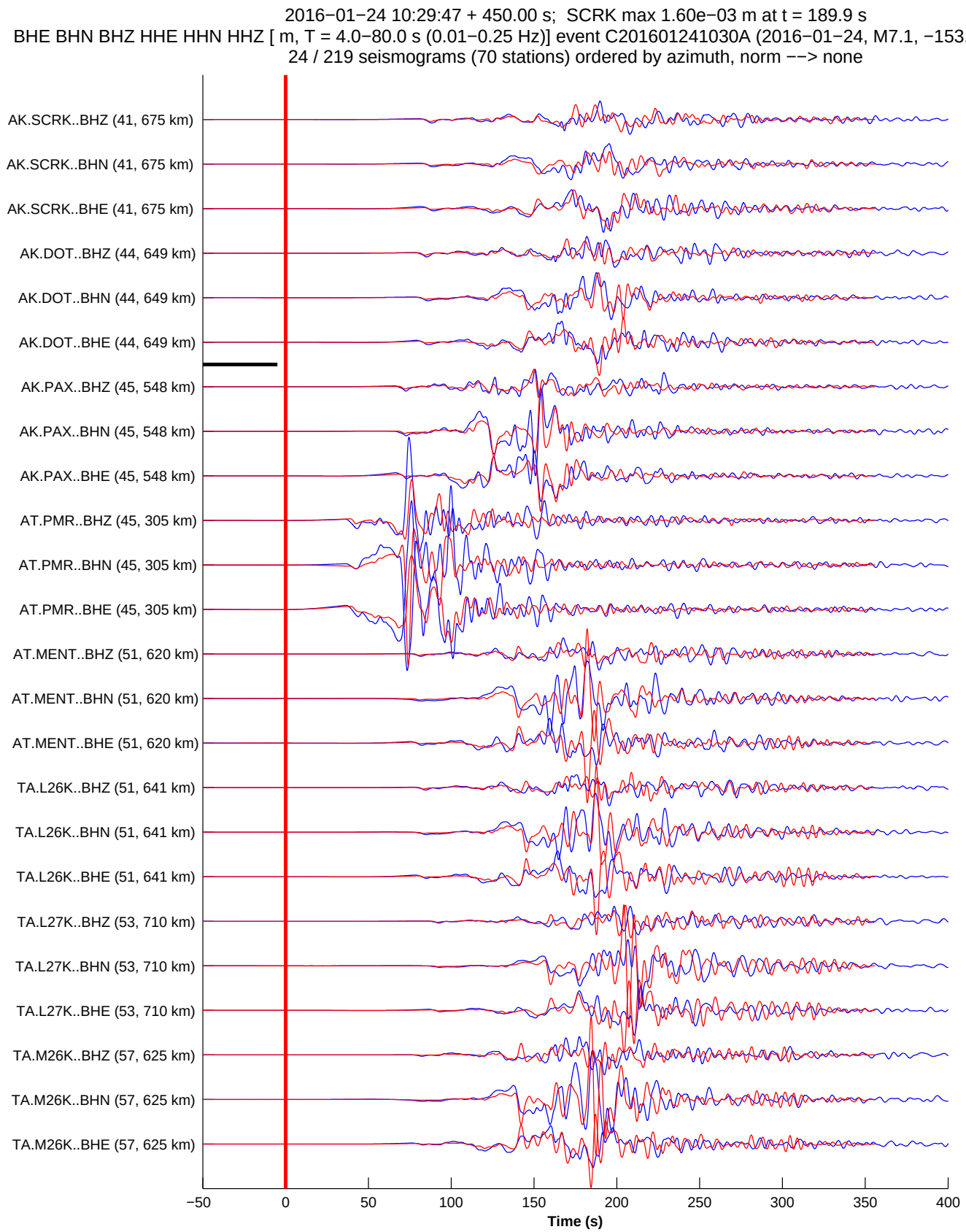

Figure 7, Part 6: station azimuths 41°–57°

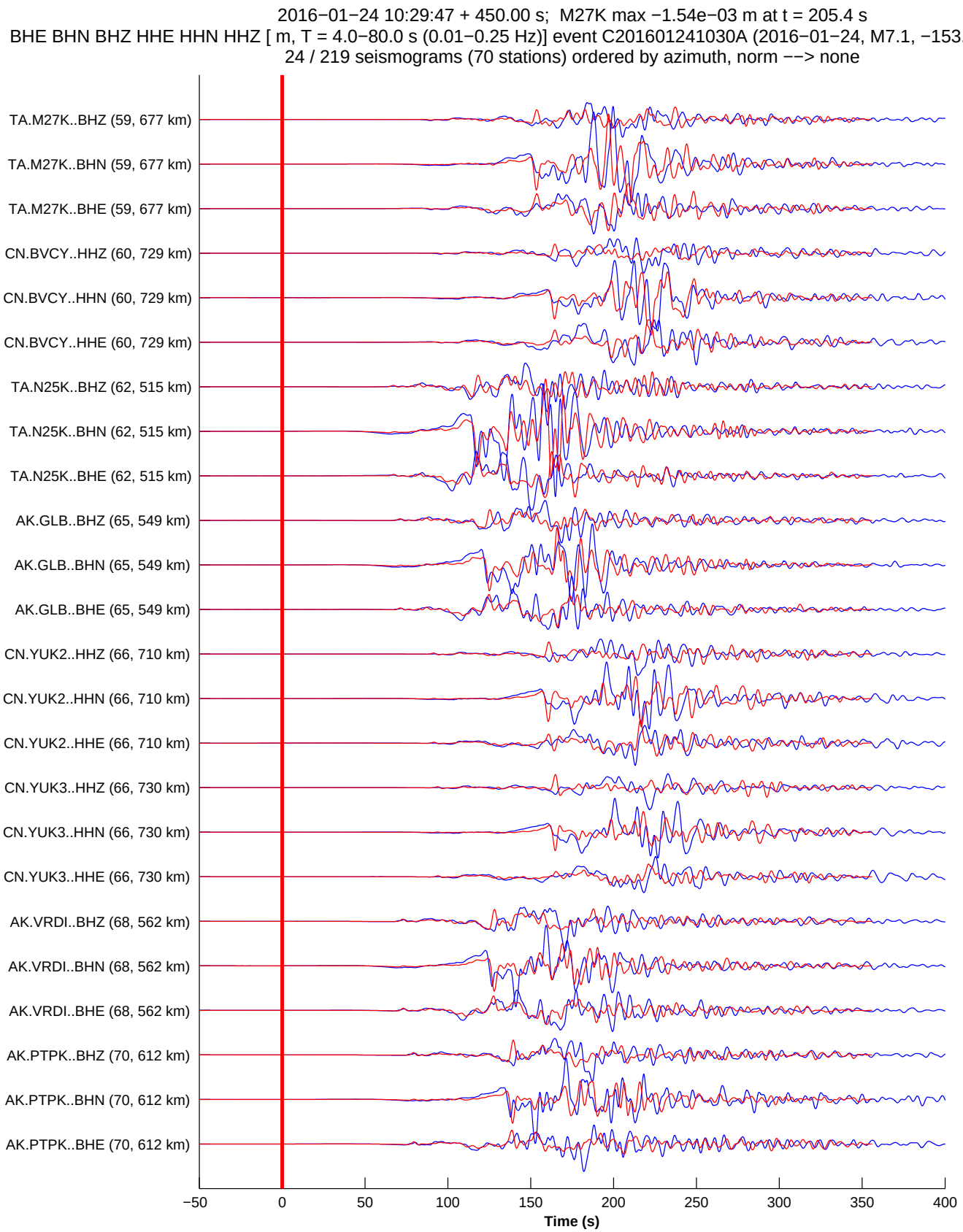

Figure 7, Part 7: station azimuths 59°–70°

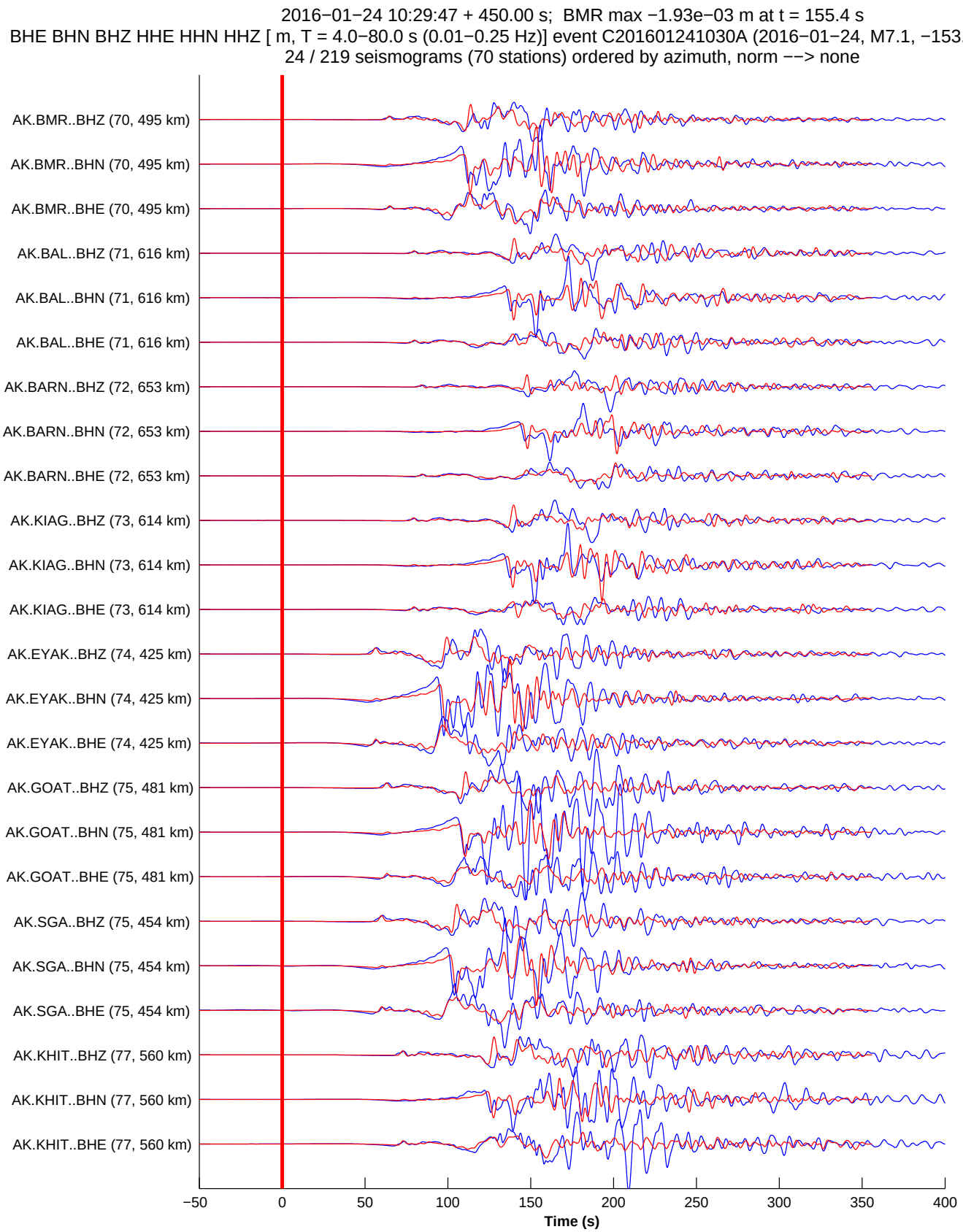

Figure 7, Part 8: station azimuths 70°–77°

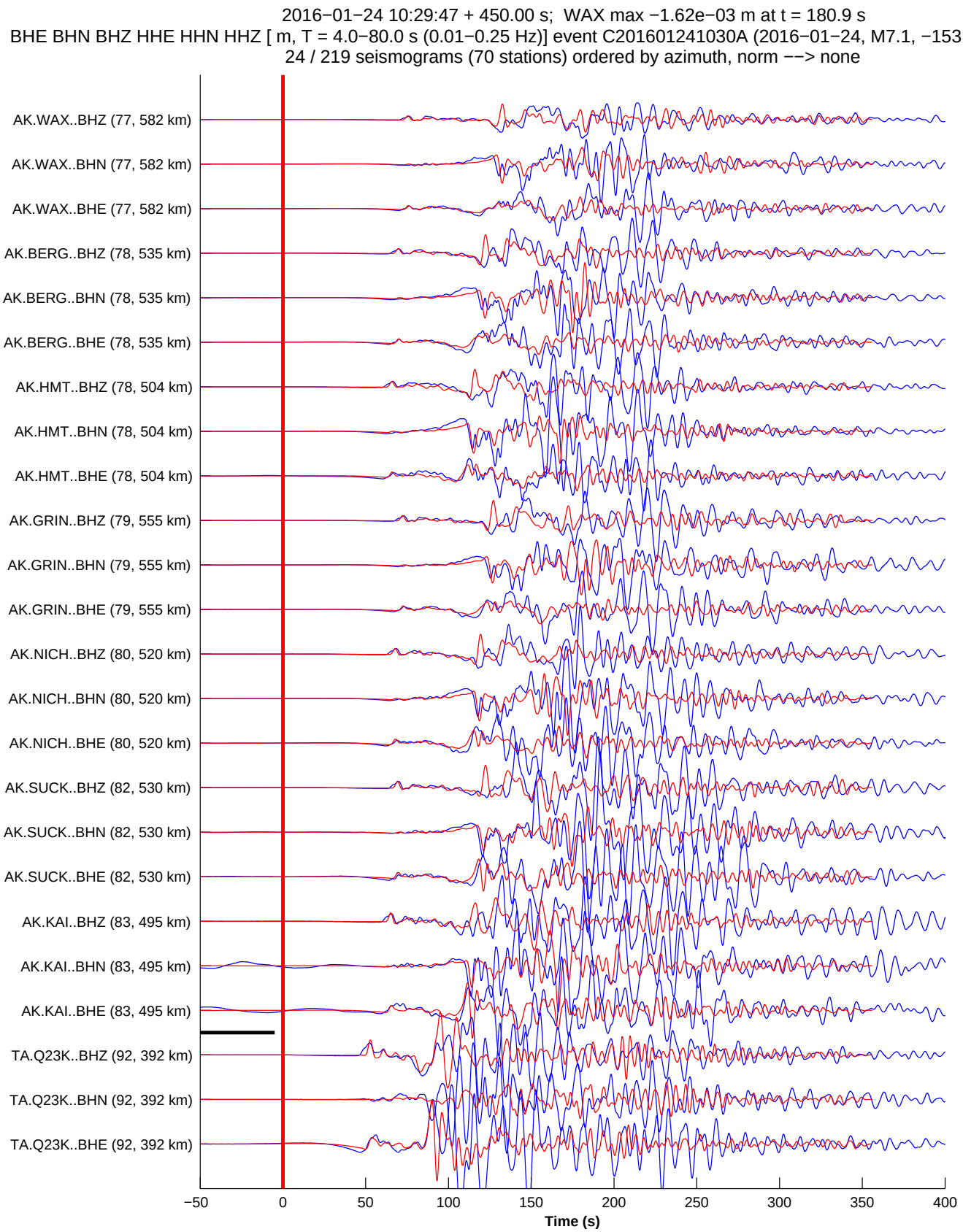

Figure 7, Part 9: station azimuths 77°–92° (large amplitudes and extended duration)

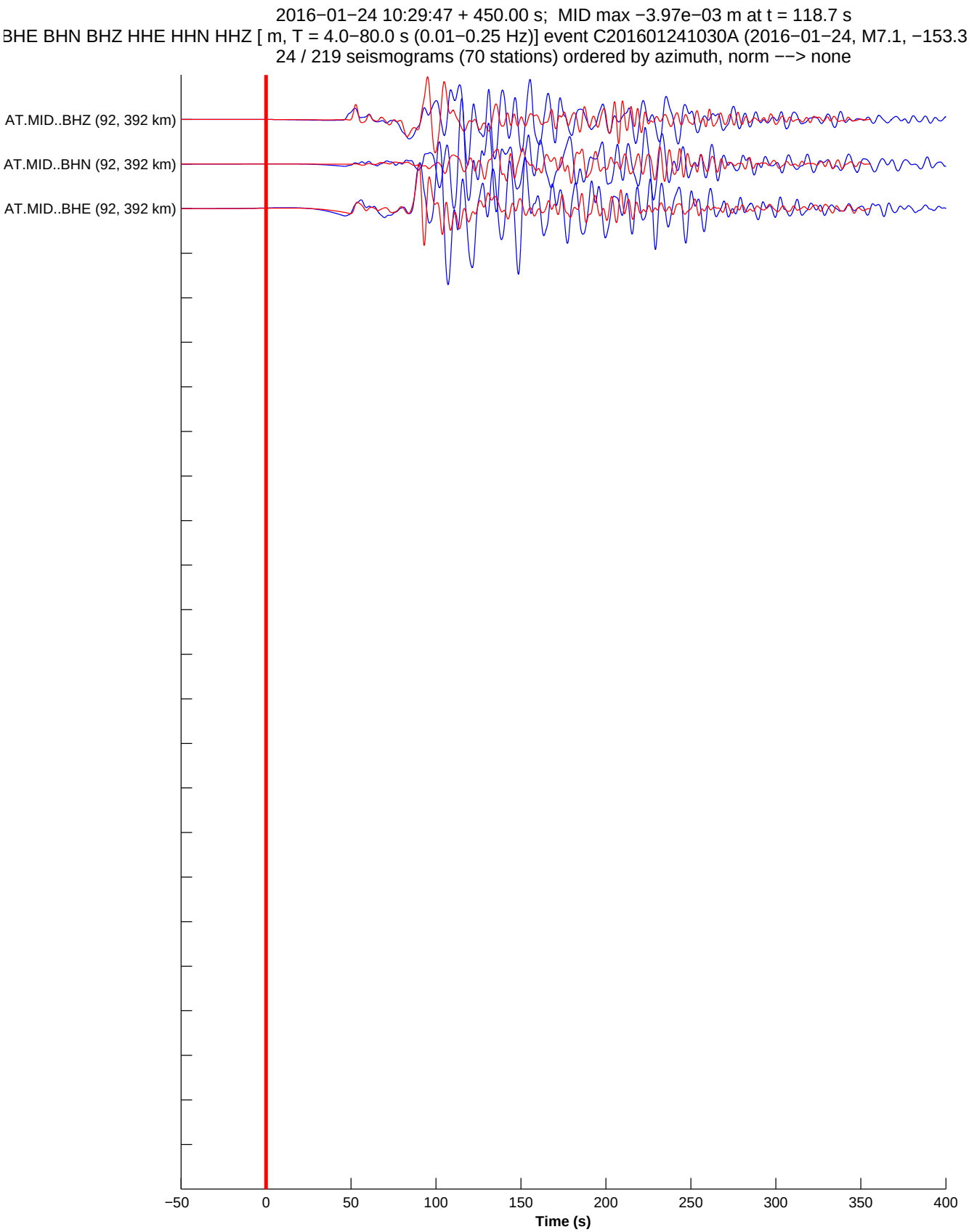

Figure 7, Part 10: station azimuths 92 (large amplitudes and extended duration)

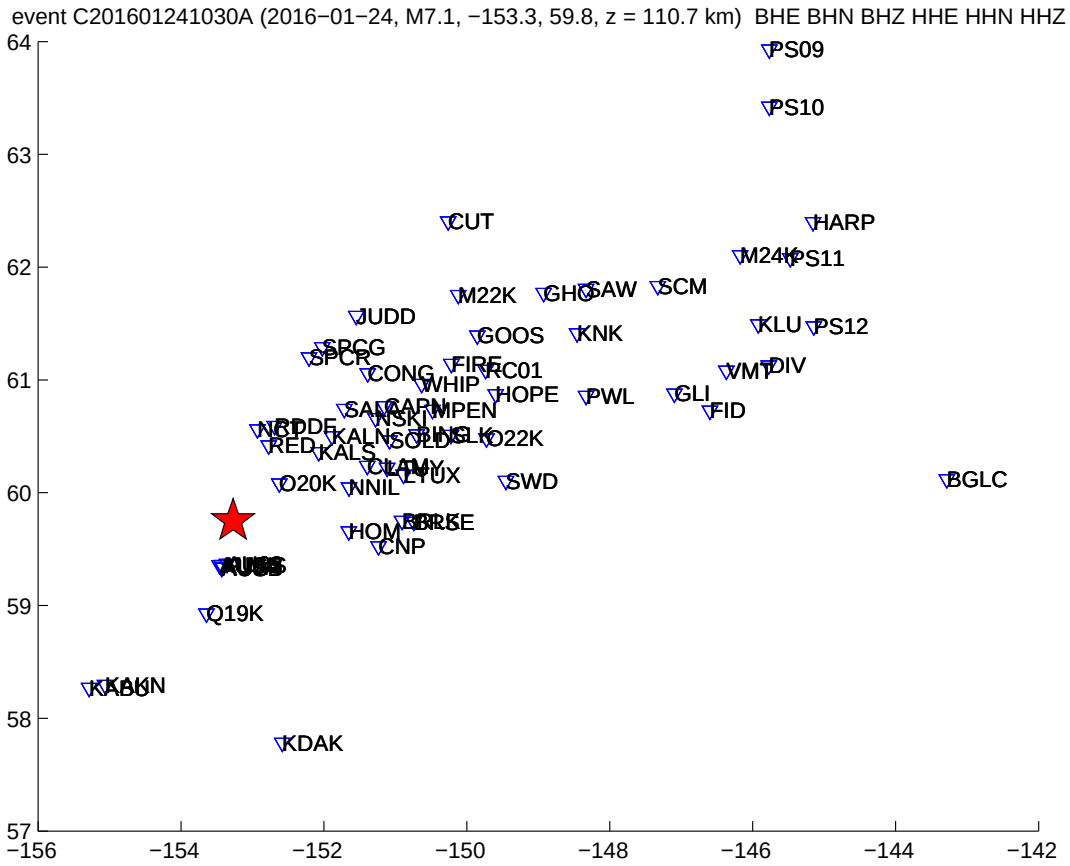

Figure 8: Map of 60 stations used in the record section in Figure 9. These are the stations with "bad" seismograms for the M_{w} 7.1 Iniskin earthquake.

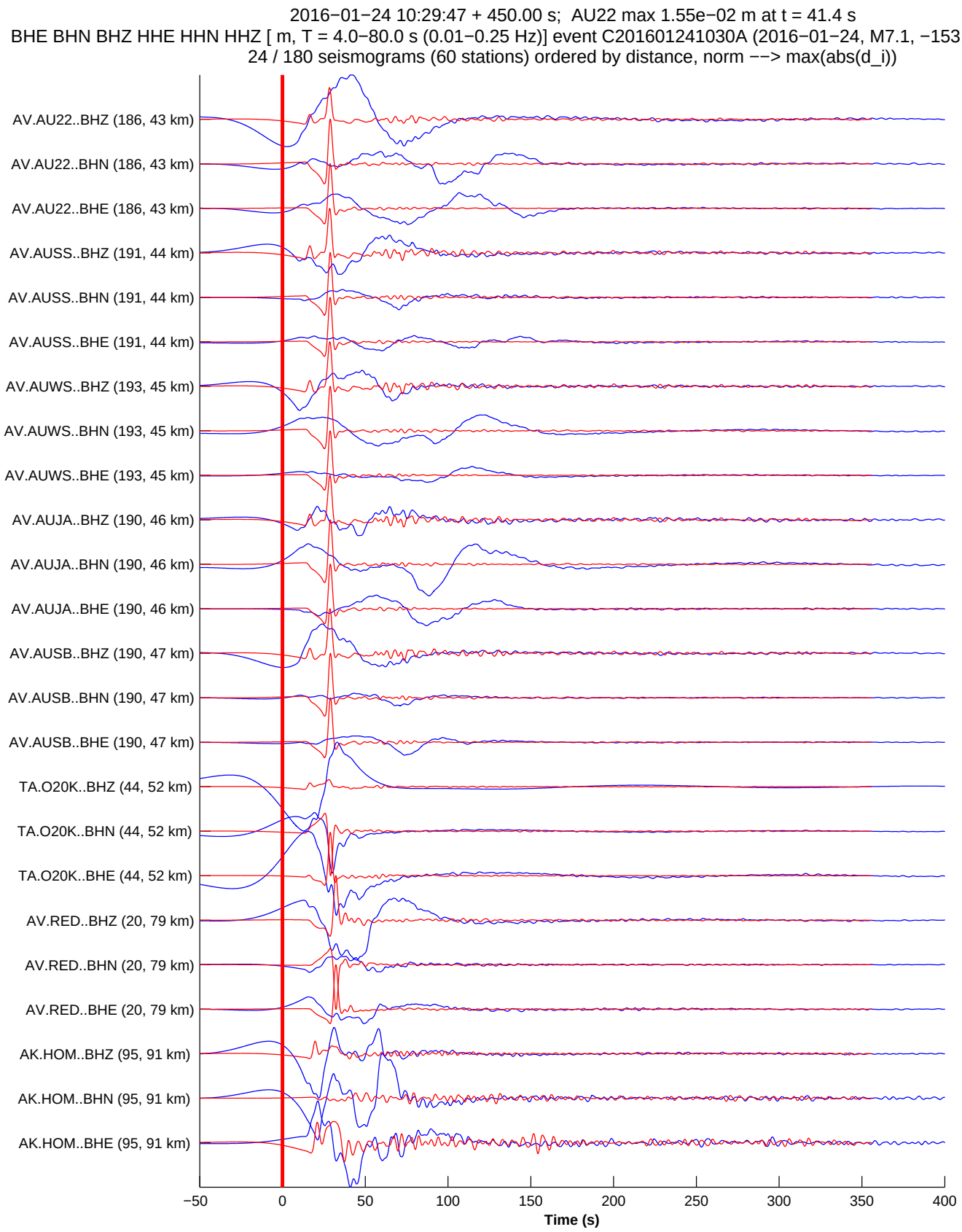

Figure 9: [CONTINUED ON FOLLOWING PAGES] All 60 stations having recorded seismograms that we deem to be bad (Table 4). Observed (blue) and synthetic (red) seismograms are filtered with periods 4–80 s, shown for all three components, and sorted by station azimuth, starting from the south. Stations are sorted by epicentral distance. **Each pair of seismograms is normalized based on the maximum value within either seismogram.**

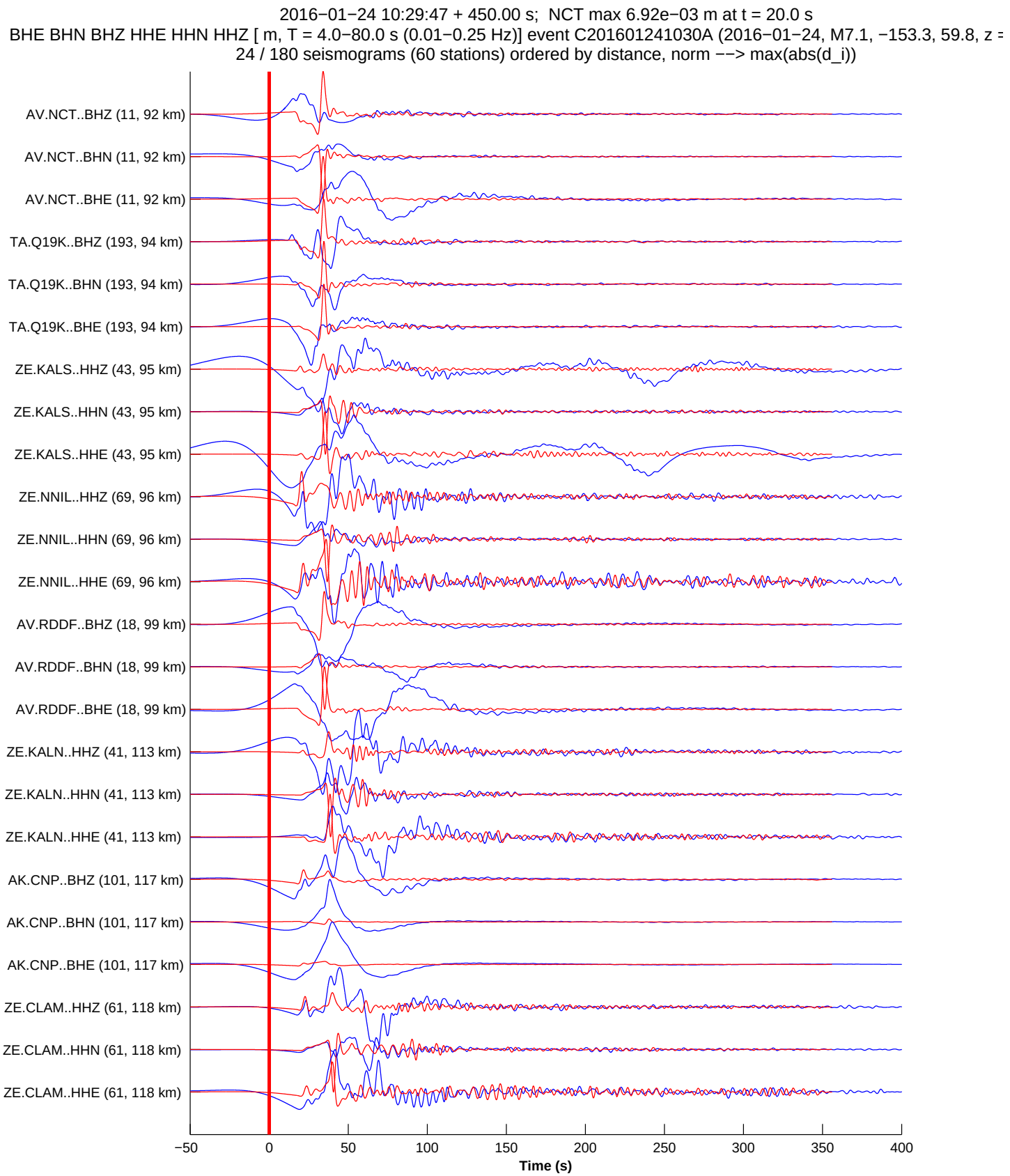

Figure 9, Part 2: station distances 92–118 km

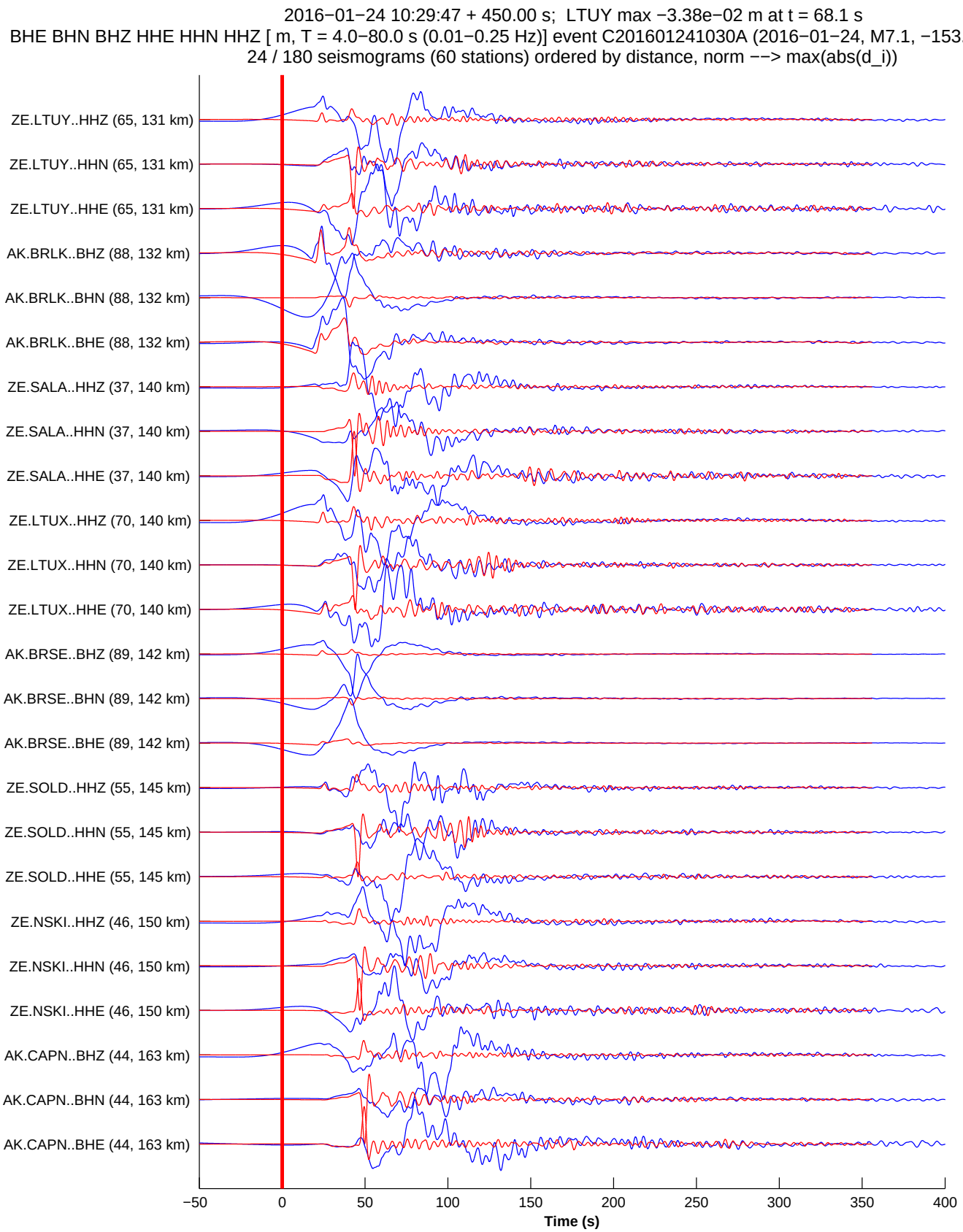

Figure 9, Part 3: station distances 131–163 km

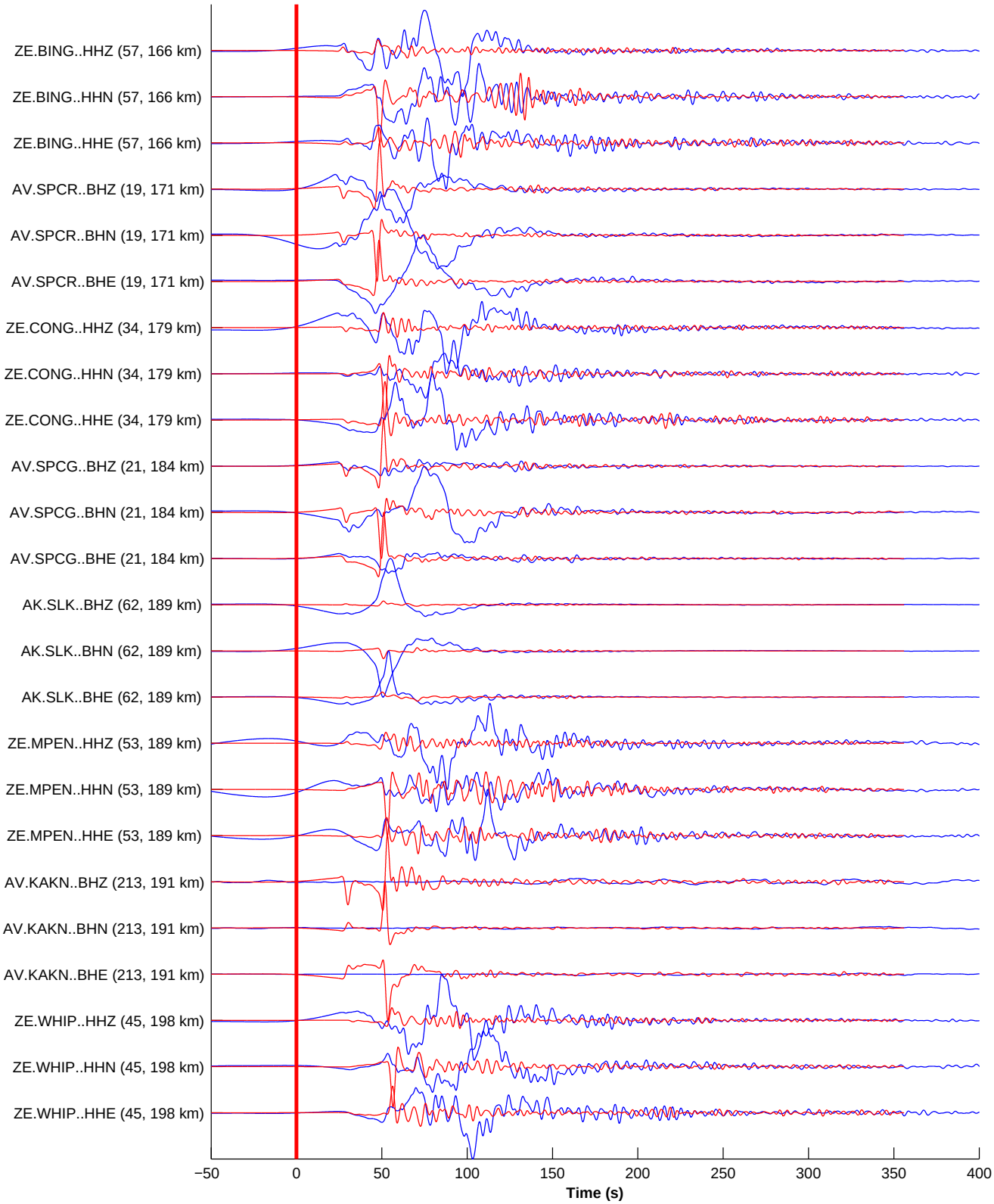

Figure 9, Part 4: station distances 166–198 km

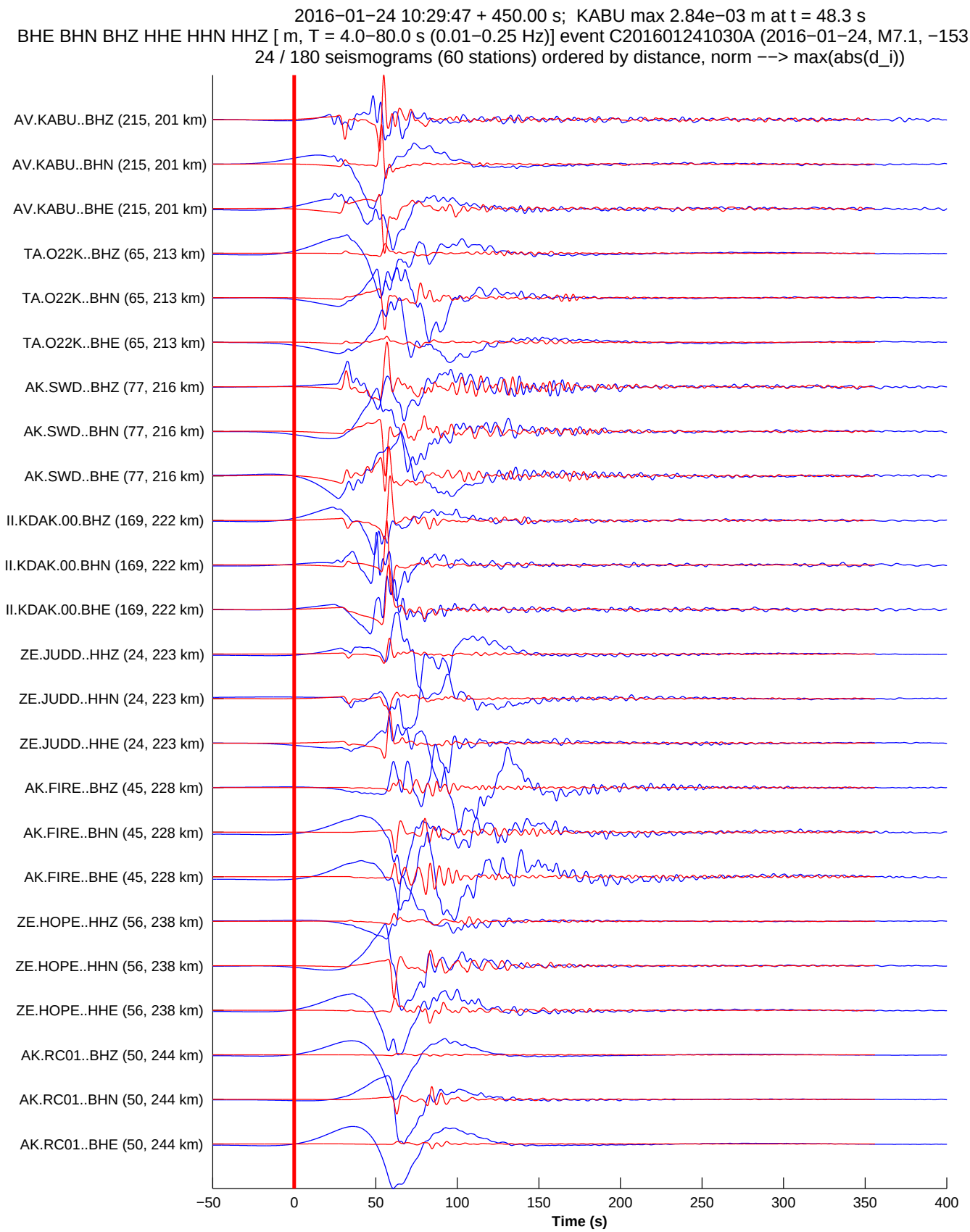

Figure 9, Part 5: station distances 201–244 km

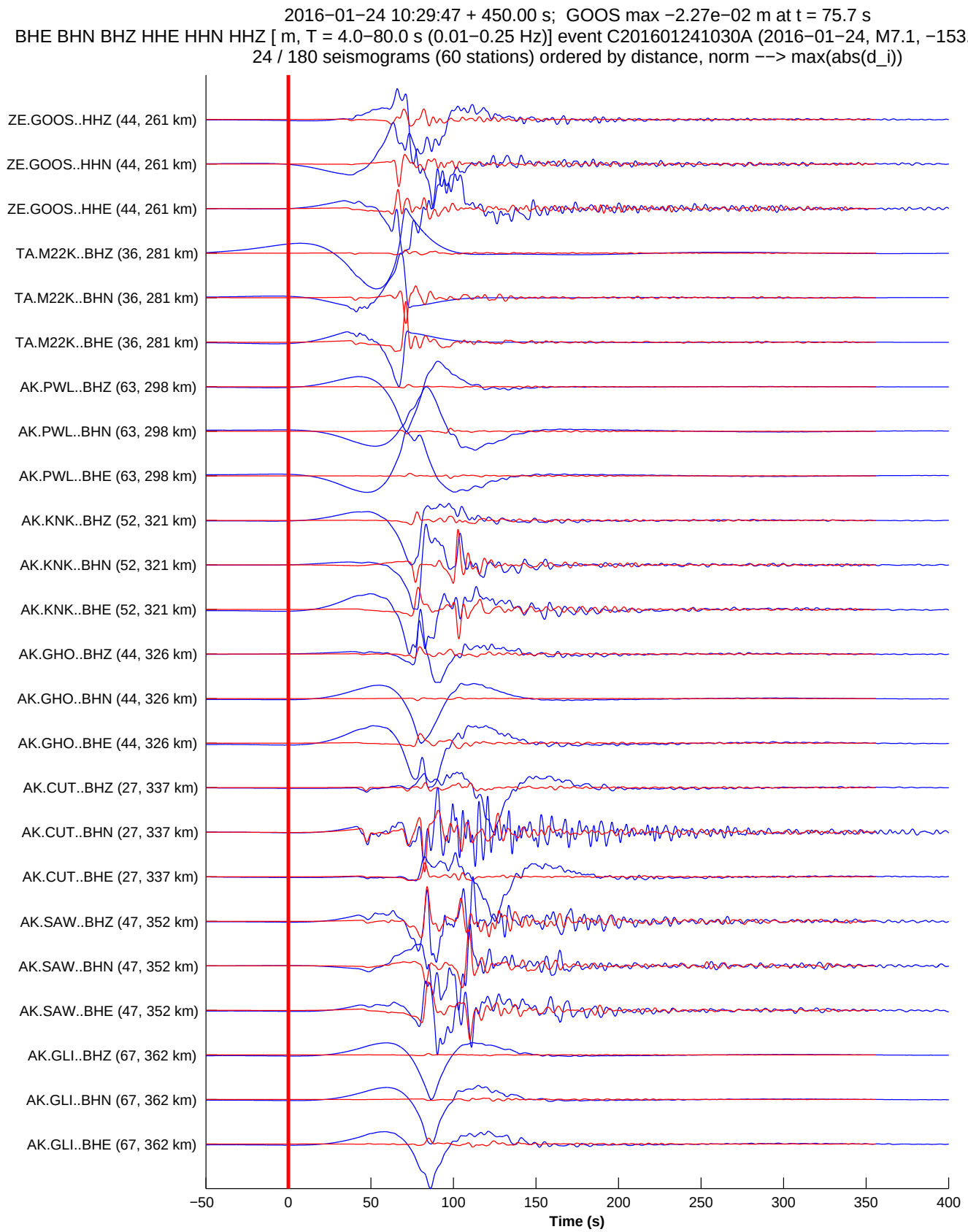

Figure 9, Part 6: station distances 261–362 km

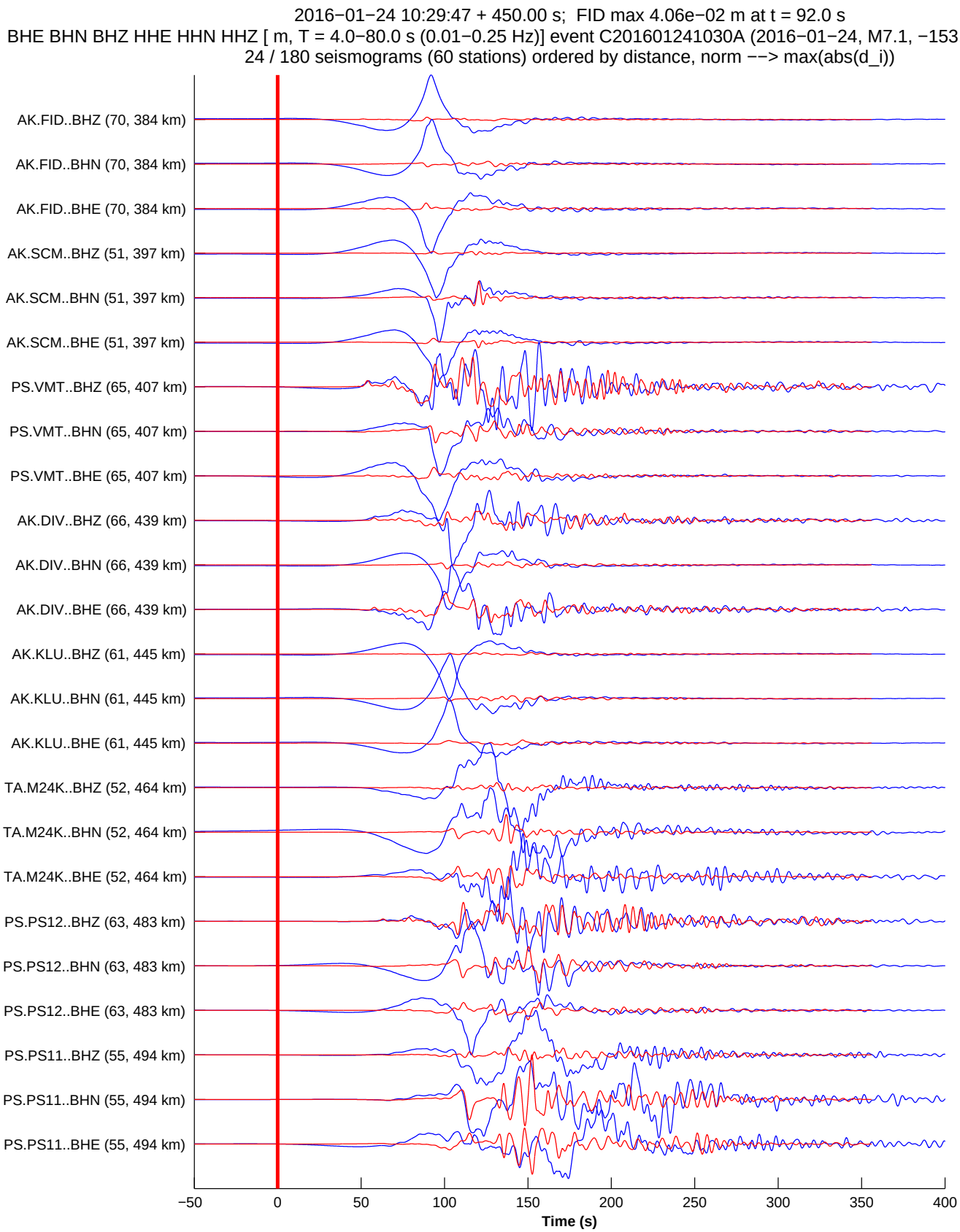

Figure 9, Part 7: station distances 384–494 km

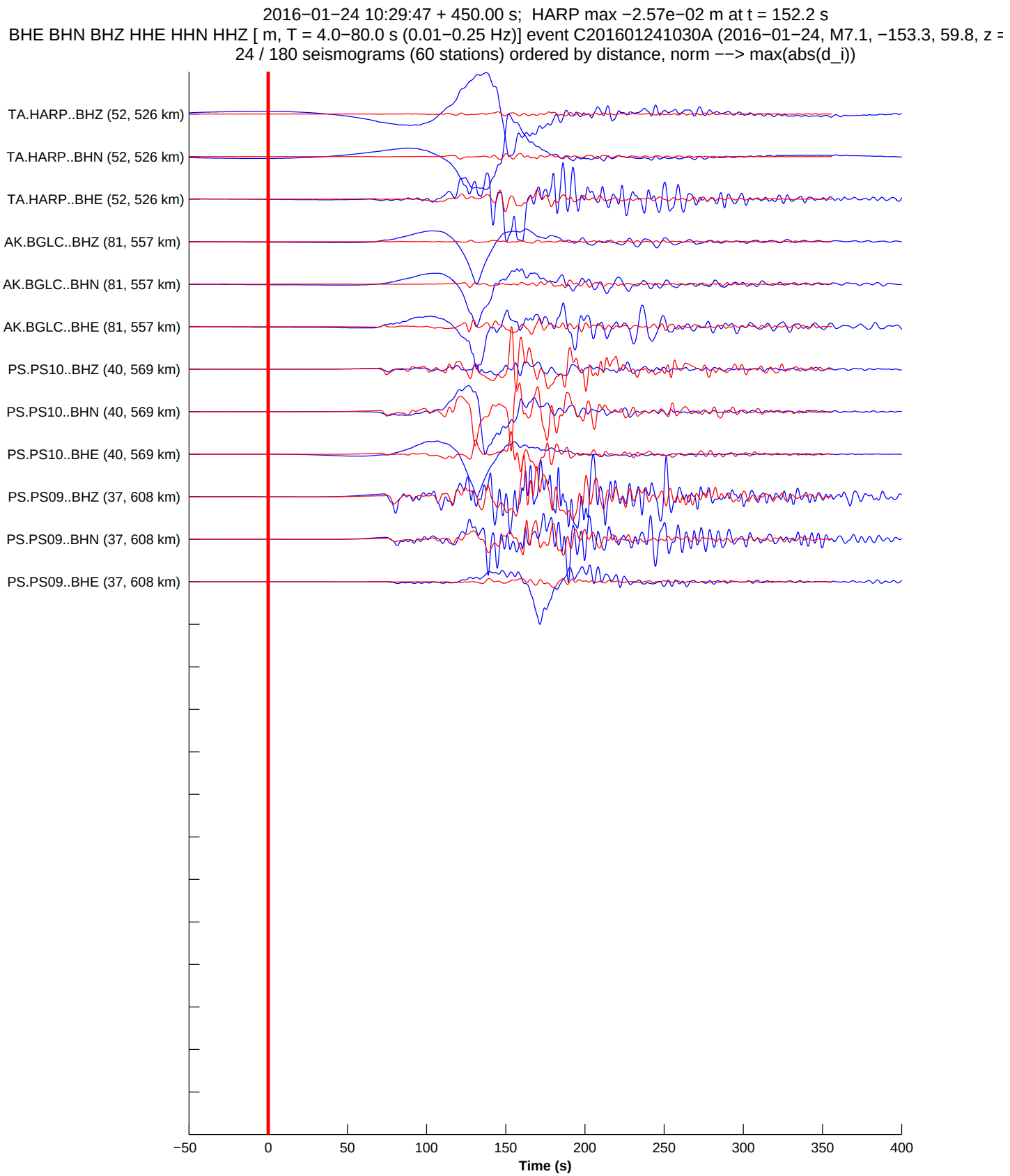

Figure 9, Part 8: station distances 526–608 km

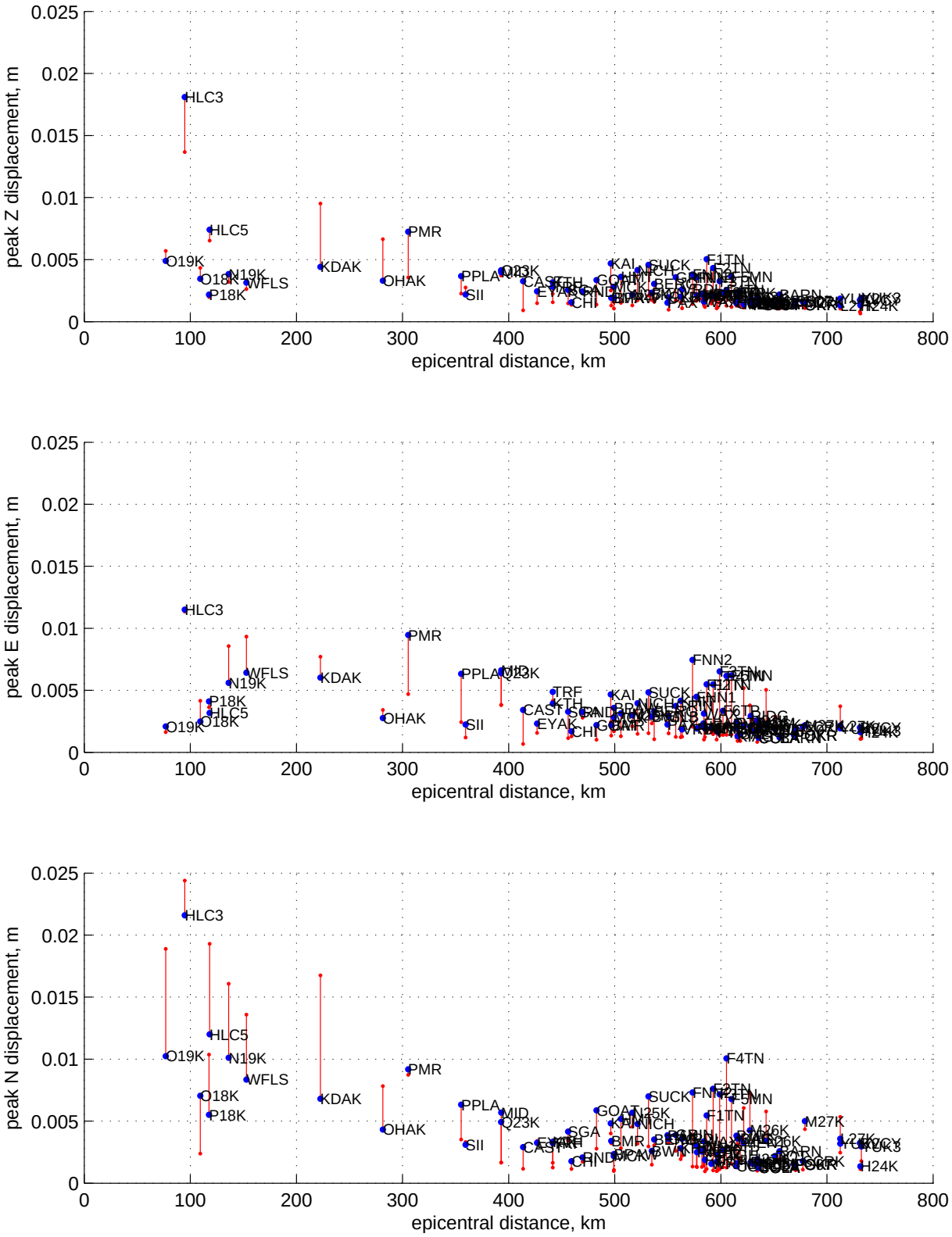

Figure 10: Comparison between peak displacements of data and synthetics for seismograms filtered between periods 4–80 s. Data amplitudes are plotted as blue dots, synthetic amplitudes are plotted as red dots, and a vertical bar connects the two. Although the plot is in terms of distance, we note that the amplitudes also depend on station azimuth, due to the influences of the source radiation pattern and to the presence of 3D structures between the source and stations. See zoomed-in view in Figure 11. Seismograms are shown in Figures 5 and 7.

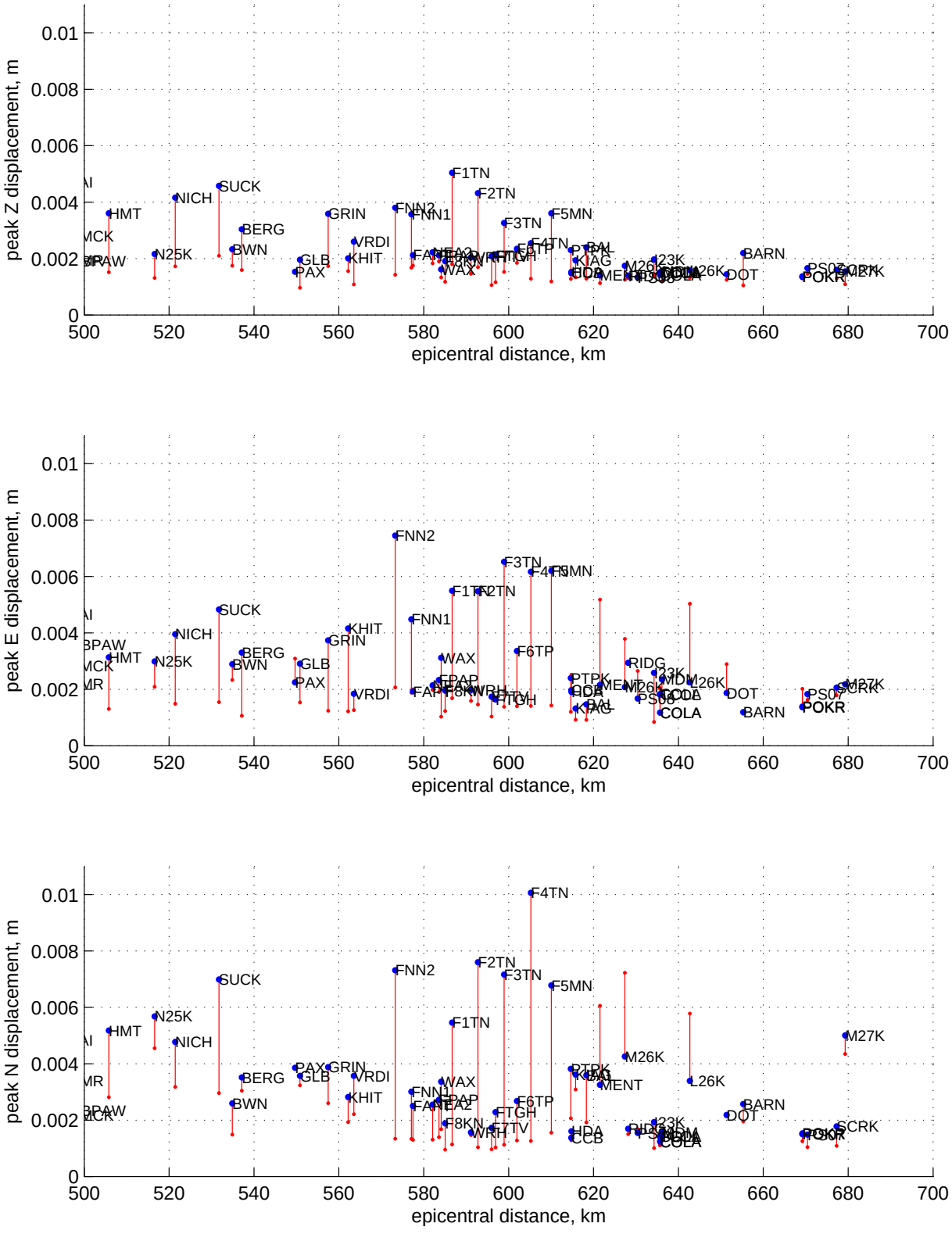

Figure 11: Same as Figure 10, but zoomed in on the epicentral distances between 500 km and 700 km.

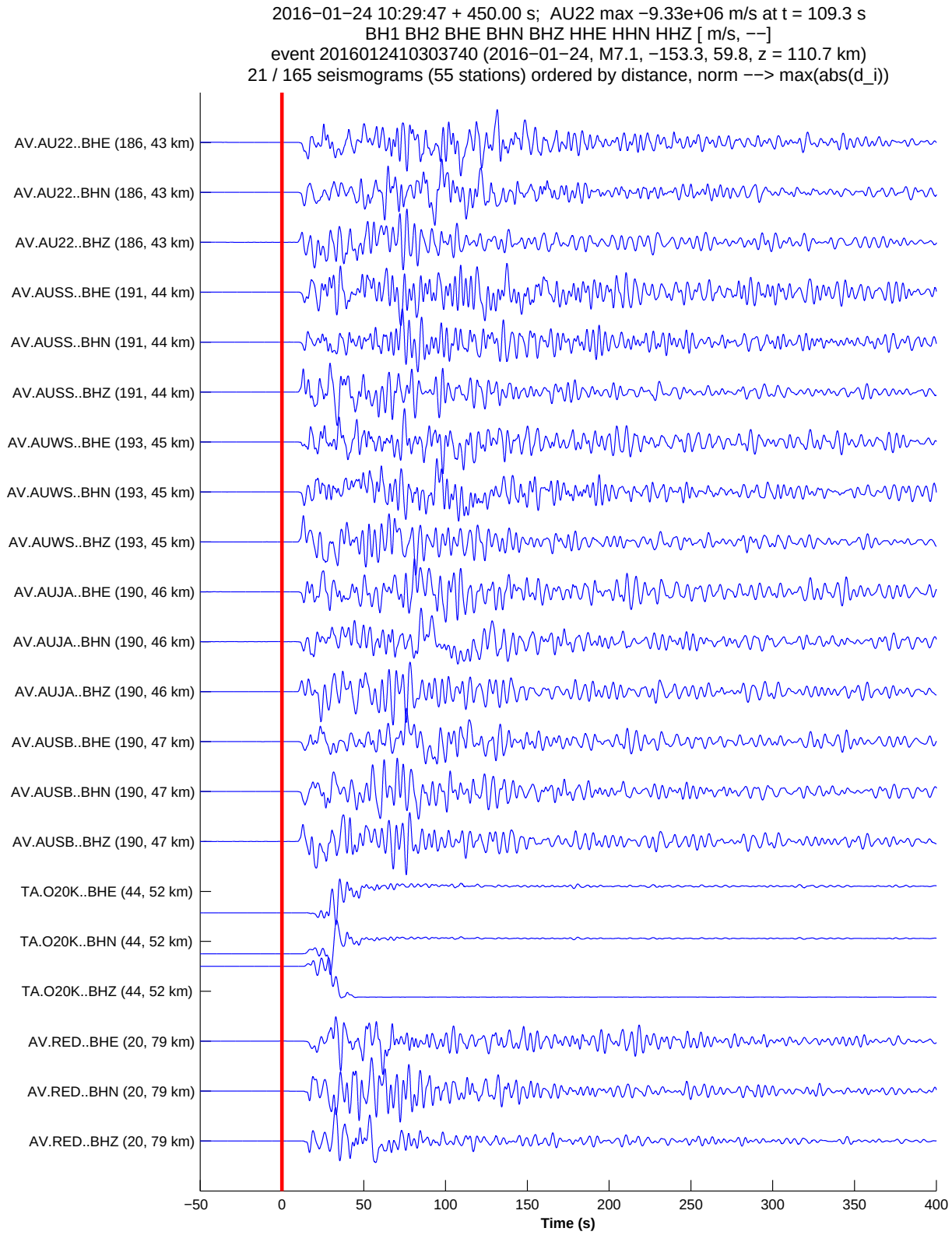

Figure 12: [CONTINUED ON FOLLOWING PAGES] All 60 stations (minus 5 pump stations: VMT, PS09, PS10, PS11, PS12) having recorded seismograms that we deem to be bad, based on comparisons between data and synthetics (Table 4). Here we plot the observed seismograms only: velocity, no removal of instrument response, no rotation to EN, and causally low-pass-filtered $T \geq 4$ s. These waveforms provide a more clear picture of the behavior of the instruments, in comparison with the filtered displacement seismograms in Figure 9. The seismograms are ordered by epicentral distance. **Each seismogram is normalized based on the maximum value of the seismogram.**

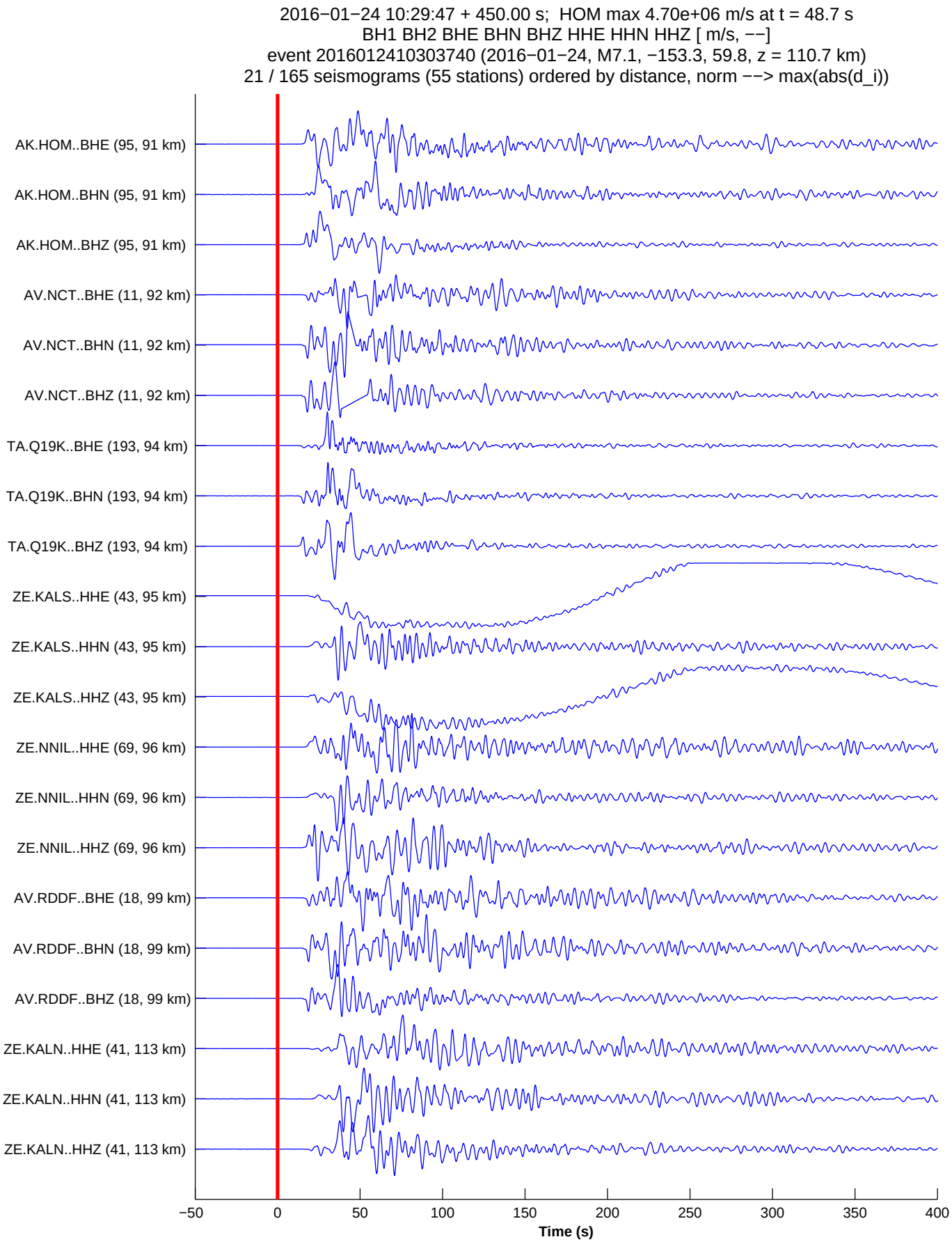

Figure 12, Part 2

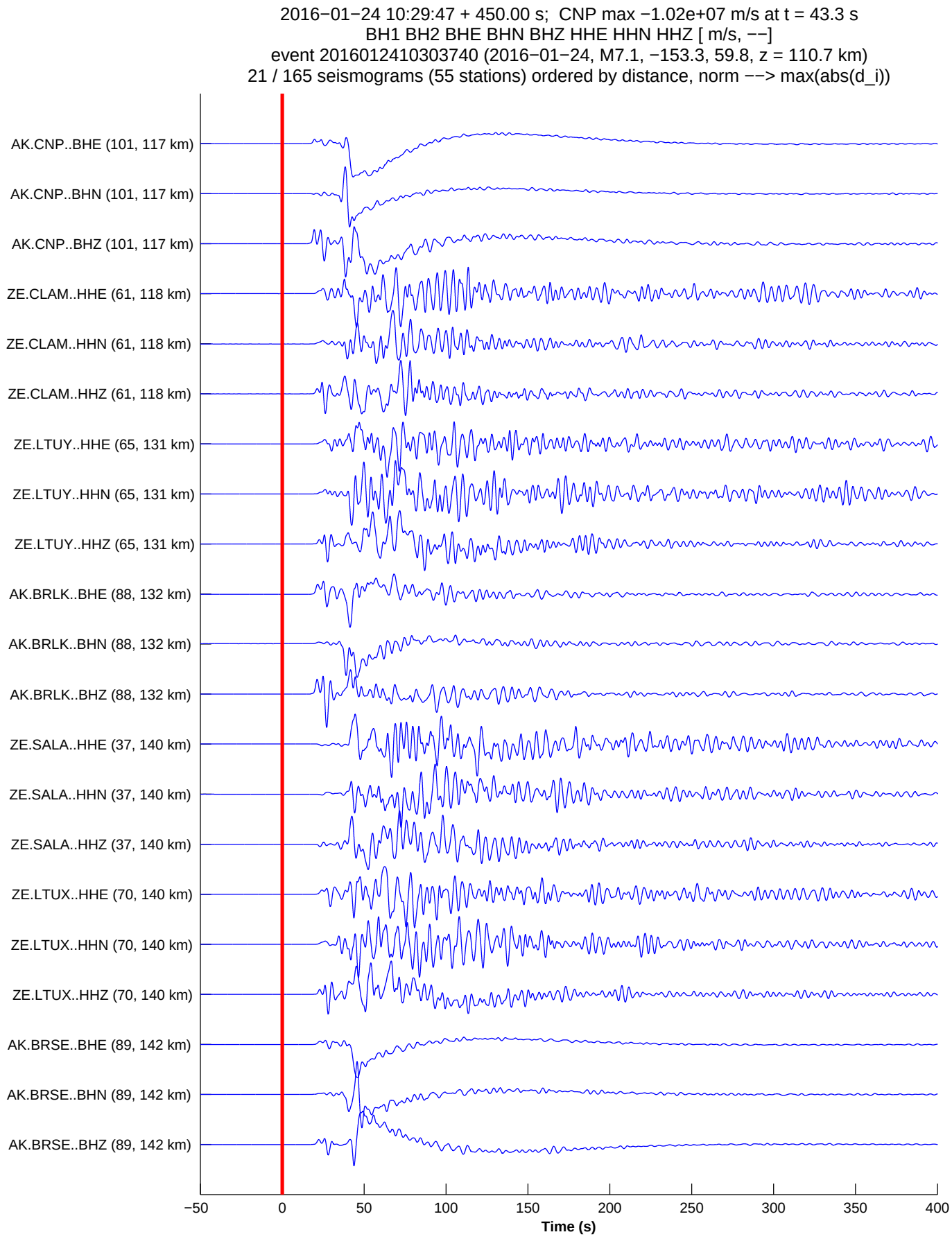

Figure 12, Part 3

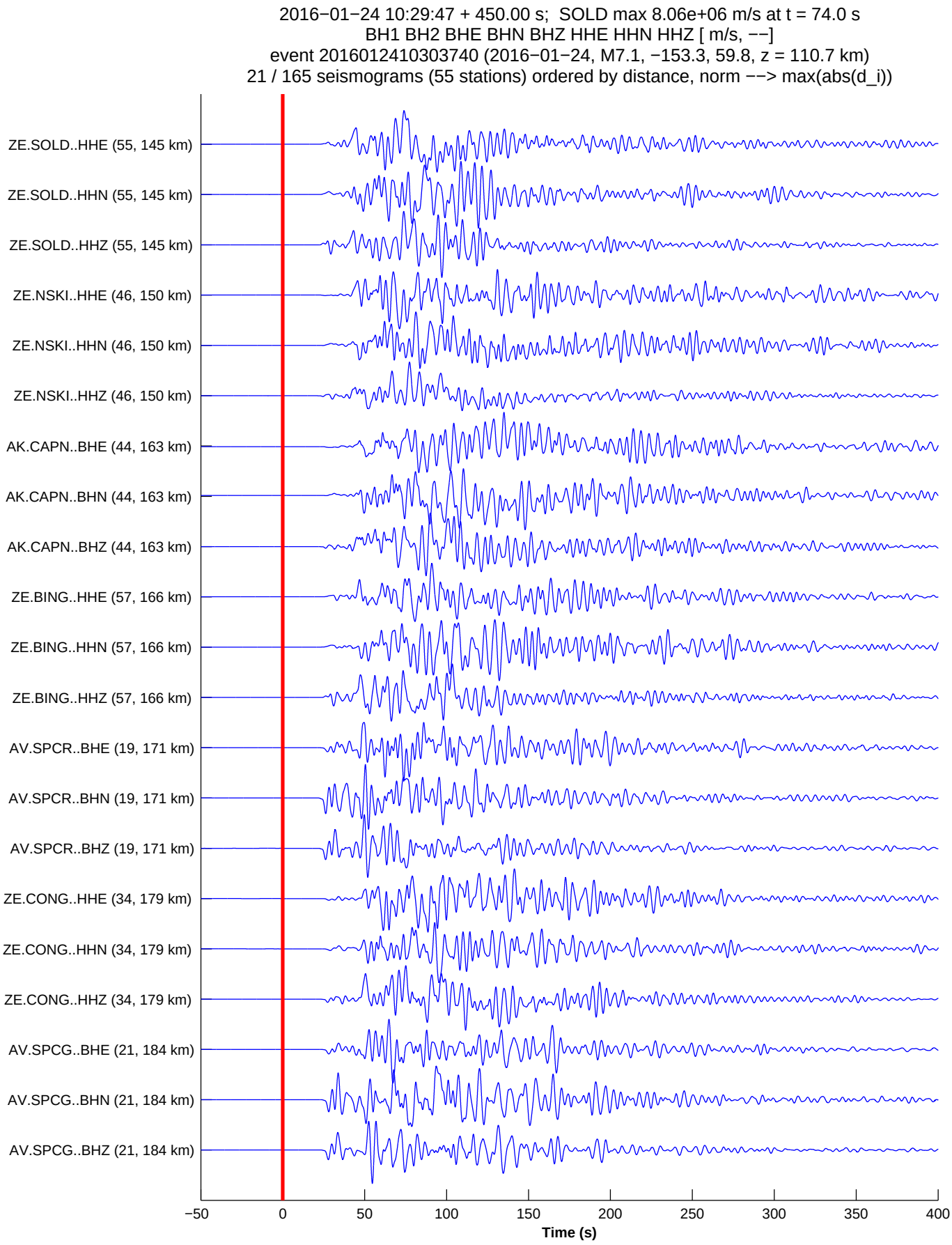

Figure 12, Part 4

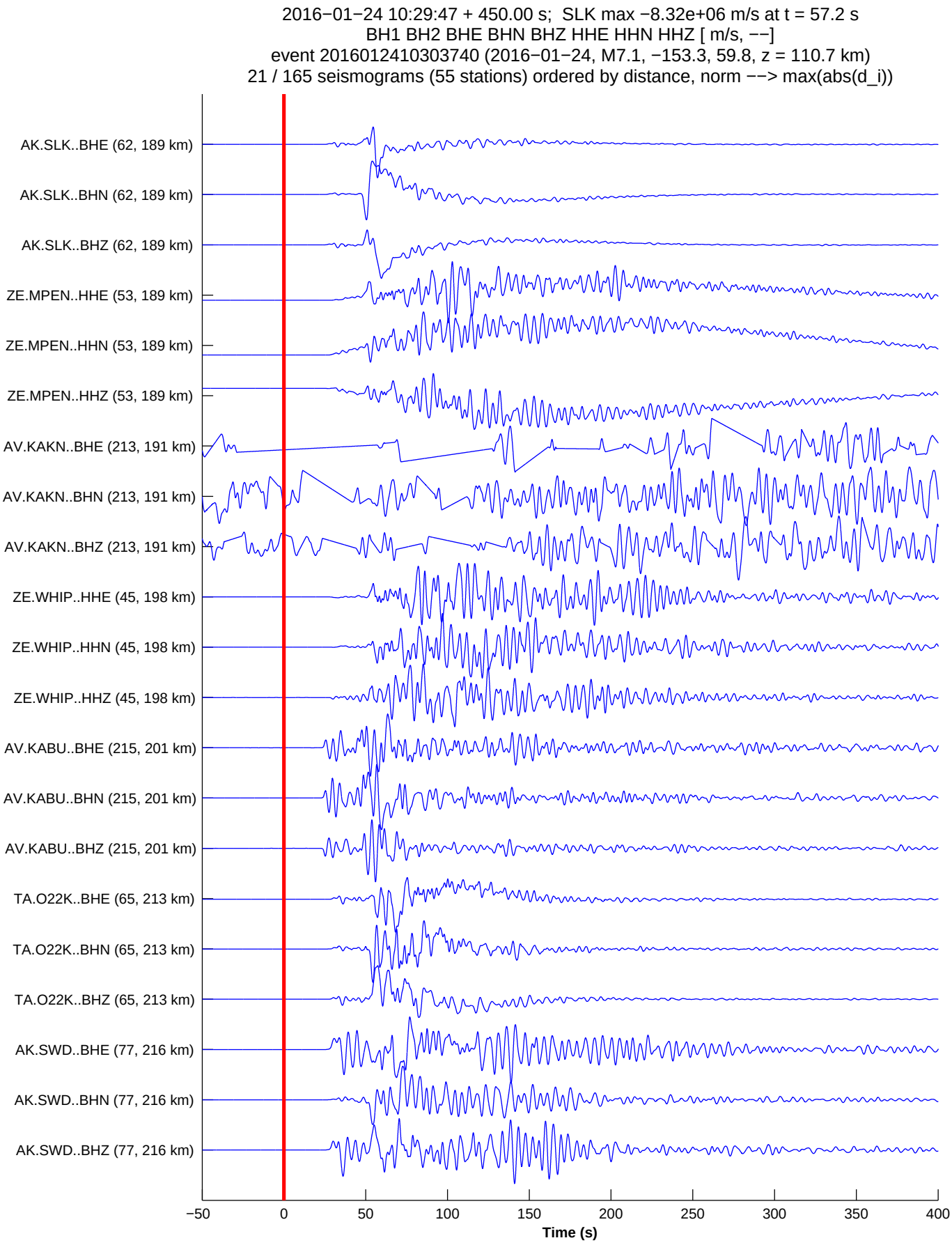

Figure 12, Part 5

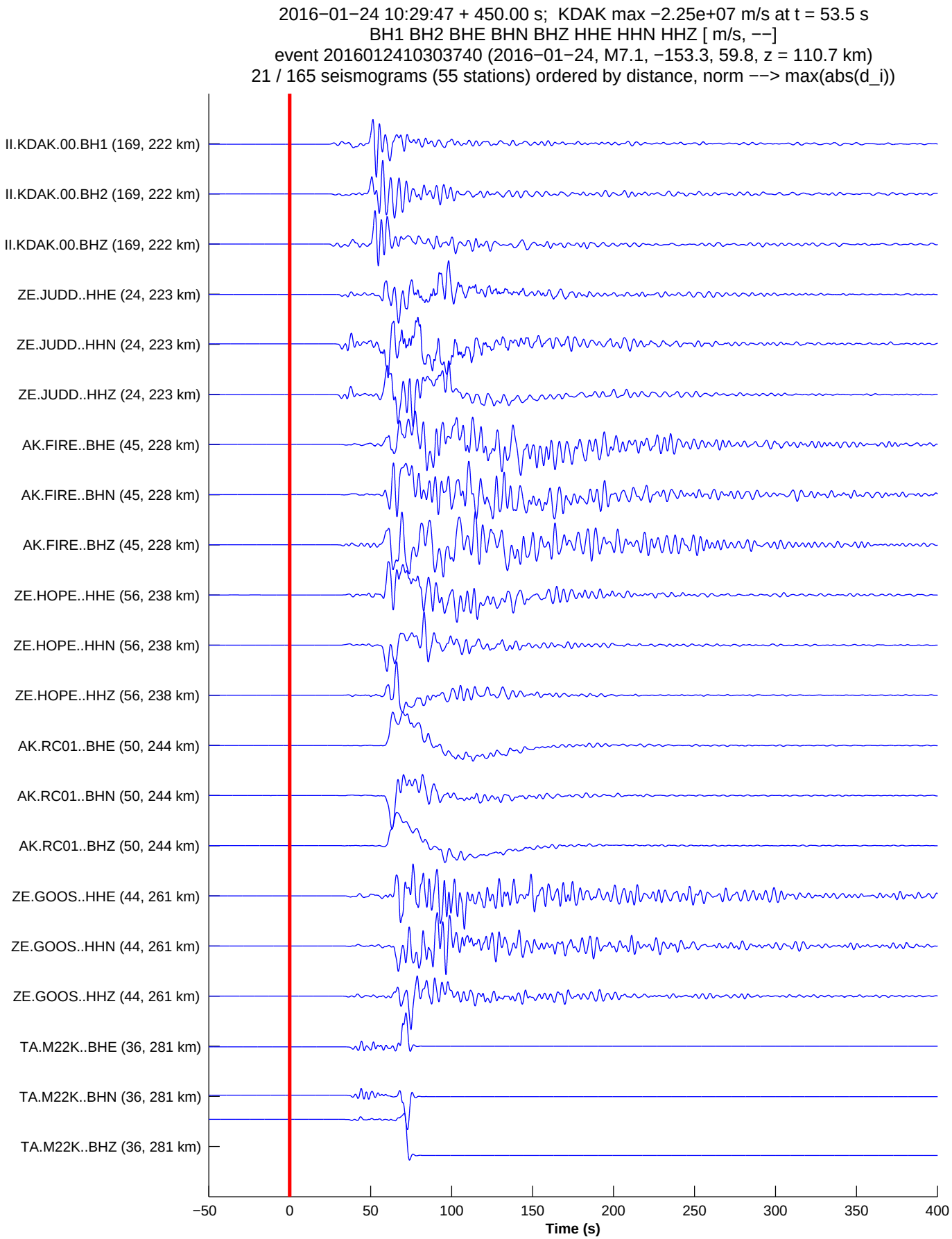

Figure 12, Part 6

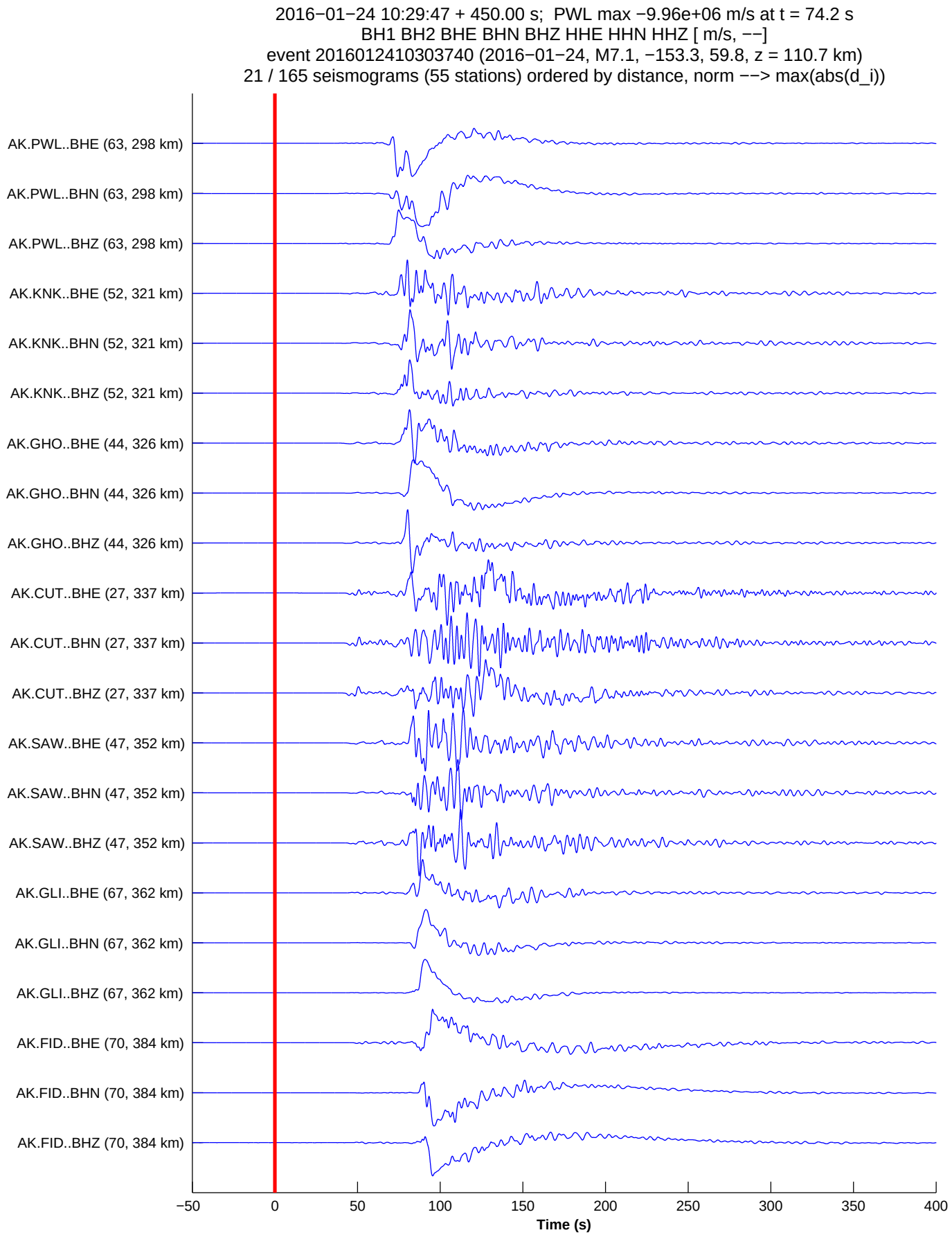

Figure 12, Part 7

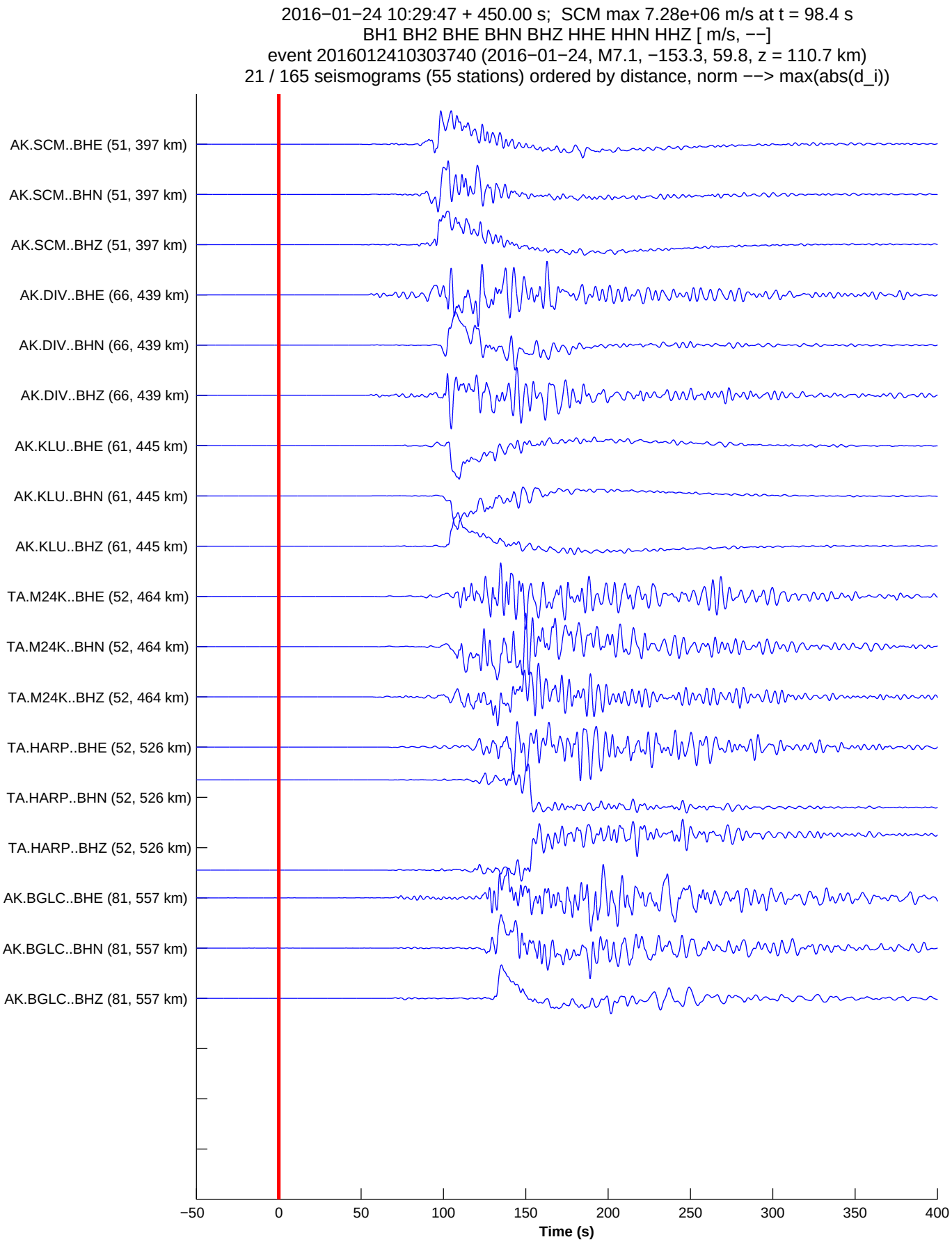

Figure 12, Part 8